Reviews of Modern Plasma Physics (2022) 6:15
https://doi.org/10.1007/s41614-022-00079-z

REVIEW PAPER

Kinetic properties of collisionless magnetic reconnection in space plasma: in situ observations

Meng Zhou[1,2] · **Zhihong Zhong**[2] · **Xiaohua Deng**[2]

Received: 31 March 2022 / Accepted: 19 June 2022 / Published online: 11 July 2022

Abstract
In collisionless plasmas, magnetic reconnection is widely recognized as one of the most important energy conversion and dissipation processes. Although reconnection is usually manifested as macroscopic effects, such as large-scale magnetic topology change and fast plasma flows, kinetic physics is the underlying process driving these macroscopic phenomena. This paper reviews the recent advances in understanding the kinetic physics in magnetic reconnection primarily on the basis of in situ satellite observations in the Earth's magnetosphere. We divide the reconnection into several sub-regions: the diffusion region, the outflow region and the separatrix region, and detail the kinetic process in these different regions. For these different regions, we start by reviewing the kinetic structure, and then discuss the particle kinetics and wave properties in these regions. Finally, we discuss some of the key unsolved questions.

Keywords Magnetic reconnection · Kinetic properties · Energy dissipation · Particle acceleration

1 Backgrounds of magnetic reconnection

Magnetic reconnection is an important energy conversion process in different plasma systems, such as space, astrophysical and laboratory plasmas. The origin idea of reconnection is proposed by Giovanelli (1946) to explain the explosive energy release phenomenon associated with solar flares. Not only converts the magnetic energy to plasma energy, but reconnection also changes the magnetic field connectivity to allow plasma from different flux tubes to mix (Dungey 1961).

✉ Meng Zhou
monmentum82@gmail.com

[1] Department of Physics, Nanchang University, Nanchang 330031, People's Republic of China

[2] Institute of Space Science and Technology, Nanchang University, Nanchang 330031, People's Republic of China

Magnetic reconnection is an important trigger for many explosive phenomena in different contexts. It is believed as the mechanism to detach the coronal mass ejection (CME) from the Sun, which is a significant release of plasma and accompanying magnetic field from the Sun's corona into the solar wind. Reconnection plays a role in the eruption of prominences and filaments, a large plasma and magnetic field structure extending outward from the Sun's surface, often in a loop shape. In the Earth's magnetosphere, reconnection is probably the driver for magnetospheric storms and substorms, which produces energetic particles in the near-Earth space and substantially disturbs the geomagnetic fields (Angelopoulos et al. 2008). Reconnection also occurs in other planets with intrinsic magnetosphere, like Mercury, and even non-magnetized planets, such as Venus. Plasmoid observation in the near Venusian magnetotail strongly supports that reconnection occurs in the Venusian magnetotail, which causes a large amount of plasma in the tail to be ejected into space (Zhang et al. 2012). In the astrophysics area, the stellar flares are similar to solar flares, which involve reconnection to release huge amounts of energy. Reconnection also occurs in pulsar magnetosphere and winds. In laboratory plasma, magnetically confined fusion such as tokamaks is used to confine a plasma to allow the nuclei in the plasma to undergo fusion; however, twisted field lines in tokamaks reconnect, limiting the plasma temperature and spoiling the device (Hesse and Cassak 2020).

Reconnection generally causes large-scale effects, including (1) large-scale magnetic topology change: particles trapped in the Earth's closed field lines can escape into the interplanetary space due to the opening of the field lines by reconnection process in the magnetosphere (Pu et al. 2013). (2) fast bulk flows: bursty bulk flows with a duration of a few minutes have frequently been observed in the magnetotail (Angelopoulos et al. 1992, 1994). These fast flows are responsible for substantial mass, momentum and energy transport (Cao et al. 2006). Bi-directional fast flows are regarded as the gold standard for identifying reconnection in observation (e.g., Phan et al. 2000). Recently, a new type of reconnection, the electron-only reconnection, has been identified in turbulence (Phan et al. 2018). Different from the standard reconnection, ions do not participate in the electron-only reconnection. One remarkable observational evidence for electron-only reconnection is the absence of ion outflow. (3) Energetic particles: particles accelerated by reconnection travels fast away from the reconnection site and populate the space (Øieroset et al. 2002; Chen et al. 2008; Zhou et al. 2016b). (4) MHD-scale magnetic structures: such as the flux transfer event (FTE) at the magnetopause and plasmoid in the magnetotail (Russell and Elphic 1978; Moldwin and Hughes 1994; Zong 2004). The scale of these structures is usually a few earth radii (R_E) to hundreds of R_E. Carrying a significant amount of magnetic flux and plasma, they impact greatly to the space environment.

One long-standing question of reconnection is how does it proceed such fast. The first proposed model to quantify the reconnection rate is the well-known Sweet–Parker model (Parker 1957; Sweet 1958). This model assumes the existence of a diffusion region, and that the plasma carries magnetic flux from the upstream inflow region into the diffusion region and flows out to the downstream outflow region. The predicted reconnection rate is inversely proportional to the Lundquist number, which is above 10^{10} in most space and astrophysical plasmas, corresponding

to a very small aspect ratio of the diffusion region. Therefore, the reconnection rate of this model is too low to explain the explosive energy release phenomena observed in space and astrophysical plasmas. Petschek (1964) revised the Sweet–Parker model by constraining the size of the diffusion region and introducing the slow shock along the separatrix to accelerate plasma. The Petschek model provides a more open exhaust channel, enabling a much faster reconnection rate than the Sweet–Parker model. However, the Petschek model is not a self-consistent model (Biskamp 1986). On the other hand, both the Sweet–Parker model and Petschek model require resistivity in the diffusion region to break field lines; however, in collisionless plasma, the collision mean free path is much larger than the typical scale of the reconnection region; hence, collisional resistivity is negligible in collisionless reconnection.

It is then realized that the Hall effect is essential for fast reconnection (Terasawa 1983). Birn et al. (2001) demonstrate that the models including the Hall effect reach a similar dimensionless reconnection rate of ~ 0.1, while the reconnection rate in MHD simulation employing uniform resistivity is much smaller. The essential idea of the Hall reconnection model is that dispersive waves with quadratic dispersion character $\omega \sim k^2$, i.e., whistler wave or kinetic Alfven wave, take over the role of Alfven wave in driving/mediating fast reconnection (Mandt et al. 1994; Birn et al. 2001). Therefore, electrons do not form bottlenecks to reconnection, that is, the reconnection rate is independent of the mechanisms breaking the field lines and is controlled by ion dynamics only (Birn et al. 2001; Drake et al. 2008; Shay and Drake 1998; Shay et al. 1999, 2001). The aspect ratio of the IDR is large enough for fast reconnection (Shay and Drake 1998).

A critical ingredient of the Hall model is the nested two-scale diffusion region: an electron-scale electron diffusion region is embedded within the ion-scale ion

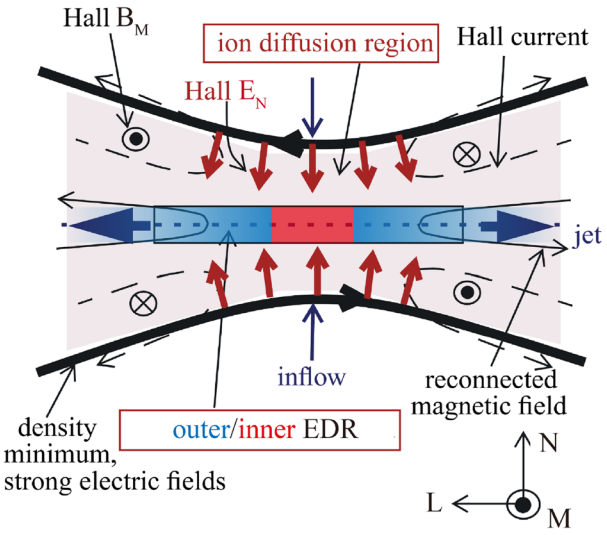

Fig. 1 The geometry of the magnetic reconnection diffusion region of the Hall fast reconnection model (adapted from Borg et al. 2005)

diffusion region (see Fig. 1). In the ion diffusion region (IDR), ions are demagnetized, because the ion gyro-radius or inertial length is larger than the variation scale of the magnetic fields, while electrons are still frozen into the magnetic field and can be treated as fluid. In the electron diffusion region (EDR), electrons are no longer magnetized. The electron frozen-in condition is violated and magnetic field lines break and reconnect in this tiny area. Note that fast reconnection is also achieved in systems without the Hall effect, such as in positron–electron pair plasma when the ion and electron temperature are equal (Bessho and Bhattacharjee 2005), or in the presence of an extremely large out-of-plane guide field that suppresses the dispersive waves (Liu et al. 2014). Therefore, it is likely that the Hall effect is a sufficient but not necessary condition for fast reconnection.

Since the reconnection is initiated in a kinetic-scale region, kinetic physics is important in reconnection. The interaction between the MHD-scale and kinetic-scale process makes reconnection essentially a multi-scale process. We should emphasize that this paper will not give a comprehensive review of reconnection, but intends to give an idea, to the best of our knowledge, of why kinetic physics is important in reconnection and how kinetic physics regulates the reconnection process primarily based on the recent in situ observations in the Earth's magnetosphere.

2 Diffusion region

2.1 Ion diffusion region

Generally, the width of the IDR is on the order of the ion inertial length (d_i), while the length of the IDR is a few to tens of d_i, which yields a dimensionless reconnection rate of $R \sim D/L \sim 0.1$. The Hall effect becomes important in the IDR, since ions are demagnetized and electrons are still frozen-in as the spatial scale approaches the ion inertial length or gyro-radius. This can be clearly seen from the generalized Ohm's law (GOL), which is deduced under the two-fluid framework

$$E + v \times B = \eta J + \frac{J \times B}{en} - \frac{\nabla \cdot P_e}{en} + \frac{m_e}{e^2 n}\frac{\partial J}{\partial t}, \tag{1}$$

where E and B are electric and magnetic fields, v is the ion bulk velocity, J is the electric current density, P_e is the electron pressure tensor, and n is the plasma number density. The terms on the right-hand side (RHS) of Eq. (1) are the resistive term, Hall term, divergence of the electron pressure tensor and electron inertia term, respectively. The resistive term is generally ignored in collisionless plasma. The Hall term is important once the spatial scale is below the ion inertial length, while the electron pressure term and inertial term become significant when the spatial scale approaches the electron gyro-radius or inertial length.

The most prominent observational feature of the IDR is the Hall electromagnetic field, which has frequently been used to identify the IDR in observation (e.g., Sonnerup 1979; Runov 2003; Borg et al. 2005; Eastwood et al. 2010). The out-of-plane magnetic field exhibits a quadrupolar structure: positive B_{M} in the quadrant with

$B_L > 0$ and $v_L > 0$ or $B_L < 0$ and $v_L < 0$, negative B_M in the quadrant with $B_L > 0$ and $v_L < 0$ or $B_L < 0$ and $v_L > 0$. The electric fields normal to the current sheet exhibit a bipolar structure across the current sheet, that is, $E_N > 0$ when $B_L < 0$ and $E_N < 0$ when $B_L > 0$. Here, the vectors are presented in the local LMN coordinate, as illustrated in Fig. 1. **L** points to the reconnecting component of the magnetic field, **N** is normal to the current sheet, and **M** is the out-of-plane direction, defined as $\mathbf{M} = \mathbf{N} \times \mathbf{L}$. The quadrupolar out-of-plane magnetic field can be simply understood by Ampere's law as there is in-plane Hall current loop. It can also be understood as the drag of magnetic field lines by the non-uniform out-of-plane electron flows (Mandt et al. 1994). The Hall electric field is mostly contributed by the Hall term in GOL. It is a polarization electric field along the current sheet normal as a result of the charge separation between ions and electrons, since electrons move deeper inside the diffusion region.

Because the ion gyro-radius is comparable to or larger than the gradient/curvature length of the magnetic field, ion velocity distribution functions (VDFs) in the IDR deviate significantly from the Maxwellian distribution, exhibiting non-gyrotropic feature in the plane perpendicular to the magnetic field (Zhou et al. 2019c). Ions (both protons and heavy ions such as oxygens) from the inflow region are ballistically accelerated by the Hall electric field in the IDR, forming the counter-streaming component in the VDF (Wygant et al. 2005). Ion VDF in the IDR also contains an energetic component, which is accelerated by the out-of-plane reconnection electric field during the ion meandering motion in the current sheet (Wang et al. 2019).

One intriguing feature of the IDR is the formation of the secondary (kinetic-scale) magnetic flux ropes (MFRs). Here, we do not strictly distinguish between the MFRs with and without evident core fields. The formation of MFRs in the thin and long current sheet has important implications for fast reconnection in the Sweet–Parker type current sheet with a large Lundquist number (Loureiro et al. 2007). A very narrow reconnection diffusion region would form in the absence of MFRs, which throttles the reconnection rate. Whereas, an elongated current sheet becomes unstable due to the growth of tearing instability and consequent formation of MFRs, which break the reconnection layer into shorter elements, then leading to a significant increase in the reconnection rate (Daughton et al. 2006, 2009; Comisso et al. 2017; Zhou et al. 2012). Secondary MFRs generated by tearing instability in the IDR have been confirmed by in situ observations (Wang et al. 2010; Huang et al. 2012a).

It is also revealed that electron Kelvin–Helmholtz (K–H) instability can also produce the secondary MFRs inside the IDR (Fermo et al. 2012; Zhong et al. 2018). The K–H instability is driven unstable by the electron jets produced by reconnection. The electron K–H vortex twists the field lines and drives secondary reconnection, finally leading to the formation of the secondary MFR. Wang et al. (2016) found plenty of ion-scale MFRs in an IDR in the magnetotail. Interestingly, those small-scale MFRs were coalescing to dissipate magnetic energy, the schematic of which is illustrated in Fig. 2. The results point out that the diffusion region in turbulent reconnection is filled with MFRs and is characterized by MFR interaction, which is consistent with 3D particle-in-cell (PIC) simulation, illustrating that the formation and interaction of MFRs due to electron physics lead the reconnection to a turbulent state (Daughton et al. 2011).

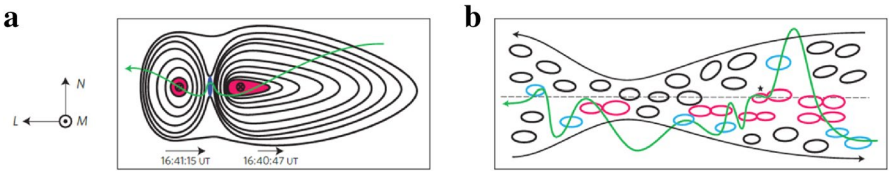

Fig. 2 Schematics for the **a** two MFRs coalescence and **b** an IDR filled by ion-scale MFRs, some of which is coalescing. Adapted from Wang et al. (2016)

Recently, sub-ion-scale magnetic holes were found in the IDR (Zhong et al. 2019, 2022). The magnetic holes are associated with electron vortex, which is commonly observed in magnetosheath turbulence (Haynes et al. 2015; Yao et al. 2017; Huang et al. 2017). The magnetic holes can be generated by electron K–H instability or the Biermann battery effect in the reconnection diffusion region (Zhong et al. 2019, 2022), and by the electron mirror mode or field-swelling instability (Gary and Karimabadi 2006; Pokhotelov et al. 2013), solitary waves (Ji et al. 2014; Yao et al. 2017), decaying turbulence (Haynes et al. 2015) in turbulence. These results suggest that these small-scale electron vortex magnetic holes contribute to energy dissipation and particle energization in reconnection and turbulence.

2.2 Electron diffusion region

As the scale approaches the electron scale near the X-line, electrons are demagnetized and magnetic fields are no longer frozen into the electron flow. This region is the EDR, where magnetic fields break and reconnect, leading to magnetic energy dissipation. Direct measurement of the EDR requires the ability to resolve the spatial–temporal scale down to the electron scale, while the unprecedented high-resolution and extremely small separation of four Magnetospheric Multiscale (MMS) spacecraft meet this requirement (Burch et al. 2016). Before the MMS era, Mozer et al. (2002) reported an EDR at the dayside magnetopause using the Polar spacecraft observations. The EDR is identified in a local minimum B region where the measured electron perpendicular flow speed deviates from the $E \times B$ drift speed, i.e., the electron slippage, which indicates the violation of the electron frozen-in condition. Furthermore, Mozer (2005) found hundreds of EDRs mainly based on the non-negligible parallel electric field at the magnetopause. Most of the EDRs were located at the separatrix region rather than the X-line; hence, those are not the classical EDRs (Mozer 2005). Nagai et al. (2011) also reported a magnetotail EDR by Geotail observations. Using the energy dissipation measure $J \cdot E' = J \cdot \left(E + v_e \times B\right)$ (Zenitani et al. 2011), Zenitani et al. (2012) quantified the energy dissipation rate as ~ 45 pW/m^3 in this EDR.

The first electron-scale measurement of the EDR is detailed in Burch et al. (2016) using the MMS observations. Figure 3 shows some main features of the EDR: intense electron-scale out-of-plane electron current (Fig. 3B), non-ideal energy conversion from electromagnetic fields to particles $J \cdot E' = J \cdot \left(E + v_e \times B\right) > 0$ (Fig. 3F) and crescent-shaped electron VDF

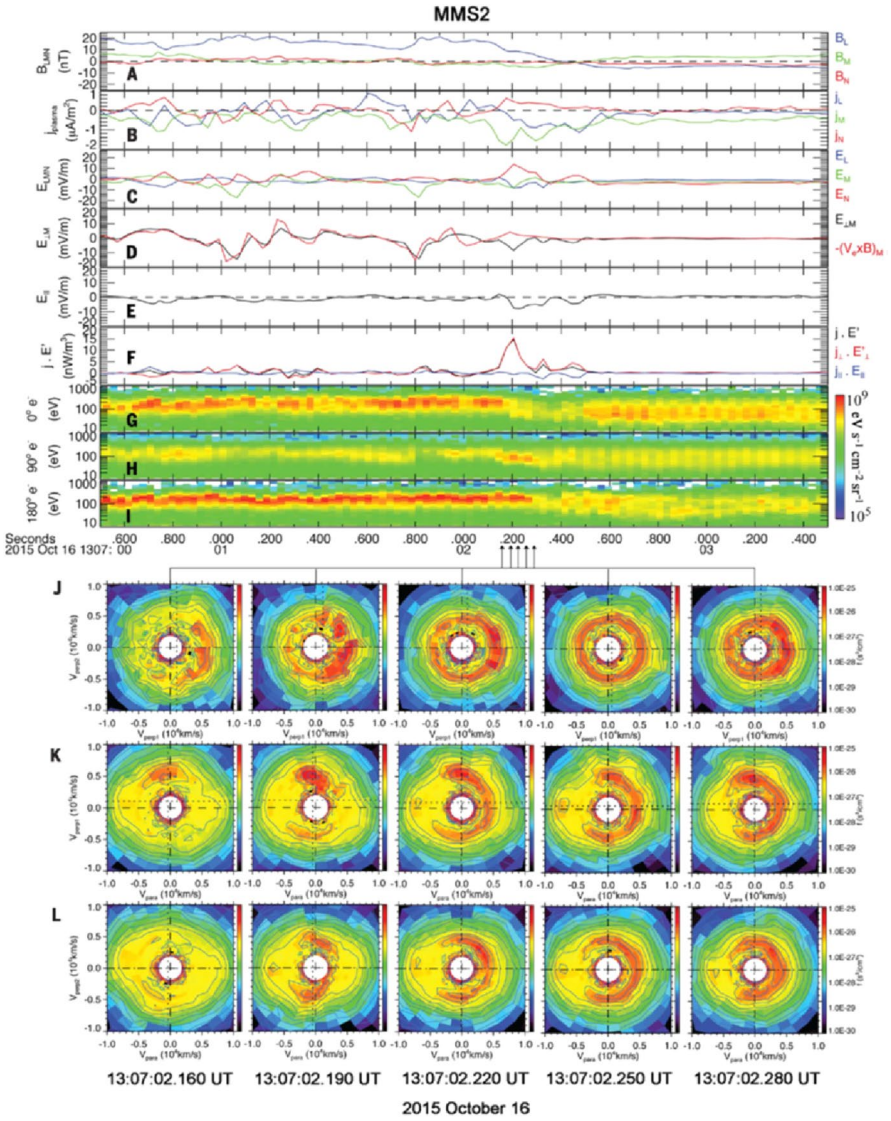

Fig. 3 An example of EDR observation by MMS at the dayside magnetopause, adapted from Burch et al. (2016). **A** Magnetic field vector. **B** Currents from plasma measurements. **C** Electric field vector. **D** Comparison of M component of E and $-V_e \times B$. **E** $E_{\parallel}$. **F** $J \bullet E$. **G** Electron energy-time spectrogram (pitch angle = 0°–12°). **H** Electron energy-time spectrogram (pitch angle = 84°–96°). **I** Electron energy-time spectrogram (pitch angle = 168°–180°). **J** Electron velocity-space distribution (V_{perp1}, V_{perp2}). **K** Electron velocity-space distribution (V_{para}, V_{perp1}). **L** Electron velocity-space distribution (V_{para}, V_{perp2}). V_{perp1} is in the $(b \times v) \times b$ direction, which is a proxy for $E \times B$

(Fig. 3J). These features serve as common criteria to identify EDR in space plasma. After that, an increasing number of EDRs were observed in magnetopause (e.g., Webster et al. 2018), the magnetotail (Torbert et al. 2018; Zhou et al.

2019b; Wang et al. 2018; Huang et al. 2018b) and the turbulent magnetosheath (Wang et al. 2021). A new type of reconnection, the electron-only reconnection, has recently been identified in turbulence (Phan et al. 2018). Different from the standard reconnection, ions do not participate in the electron-only reconnection. One remarkable observational evidence for electron-only reconnection is the absence of ion outflow.

The crescent-shaped VDF (shown in Fig. 3J, two leftmost panels) in the plane perpendicular to the ambient magnetic field is a compelling signature of the EDR in both the symmetric and asymmetric reconnection with a weak guide field (Burch et al. 2016; Torbert et al. 2018; Zhou et al. 2019b), which is formed due to meandering motion of electrons in an electron-scale field reversing layer (Hesse et al. 2014; Lapenta et al. 2017), or finite Larmor radius effect of well-magnetized electrons (Egedal et al. 2016). Note that the electron VDF perpendicular to the magnetic field can be well organized by a large guide field (Zhou et al. 2017). Additionally, a crescent-shaped velocity distribution is also formed in the parallel direction near the EDR (Fig. 3K and L), probably caused by the fast field line topology change. In the exhaust close to X-line, newly reconnected field lines move rapidly away from the X-line. It is likely that these dynamics in the exhaust are responsible for the redirection of the perpendicular crescents into the observed parallel crescents (Burch et al. 2016).

Balance of the GOL or electron momentum equation in the EDR is essential for understanding how does the field lines break around the X-line. This is one of the most important and challenging issues in reconnection. Torbert et al. (2016) demonstrates that the GOL is not balanced in one EDR observed by MMS at the dayside magnetopause. They suggest that the residuals of the non-ideal electric field may be contributed by the anomalous resistivity provided by wave–particle interactions. Webster et al. (2018) also performed Ohm's law analysis in several magnetopause EDRs, in which they show that the divergence of the electron pressure term usually dominates the non-ideal terms and is much more turbulent on the magnetosphere versus the magnetosheath side of the EDR; however, there are still significant non-ideal electric field residuals. 3D kinetic simulations demonstrate that anomalous effects are important in balancing the reconnection electric field in turbulent reconnection (Che et al. 2011; Price et al. 2016). On the other hand, Egedal et al. (2018) analyzed a quasi-laminar reconnection event in the magnetotail. They found that the electric field in the EDR can be roughly balanced by the divergence of the electron pressure term, mainly by the non-gyrotropic term, consistent with the previous 2D PIC simulation (e.g., Hesse et al. 1999; Pritchett 2001). These contradictory results leave the mechanism of breaking magnetic field lines and maintaining fast reconnection still an open question.

Recent observations show that EDR may not be a single layer inside the IDR as depicted in the traditional scenario. It can be multiple layers separated in the normal direction, as shown in Fig. 4 (Zhong et al. 2022). It is suggested that the stacked EDRs are generated by the oblique tearing instability, consistent with the results from a 3D PIC simulation (Liu et al. 2013b). Interestingly, electron K–H vortices are also excited within the IDR (Fig. 4i) by the intense electron flow shear between these stacked EDRs. This suggested that both the oblique tearing instability

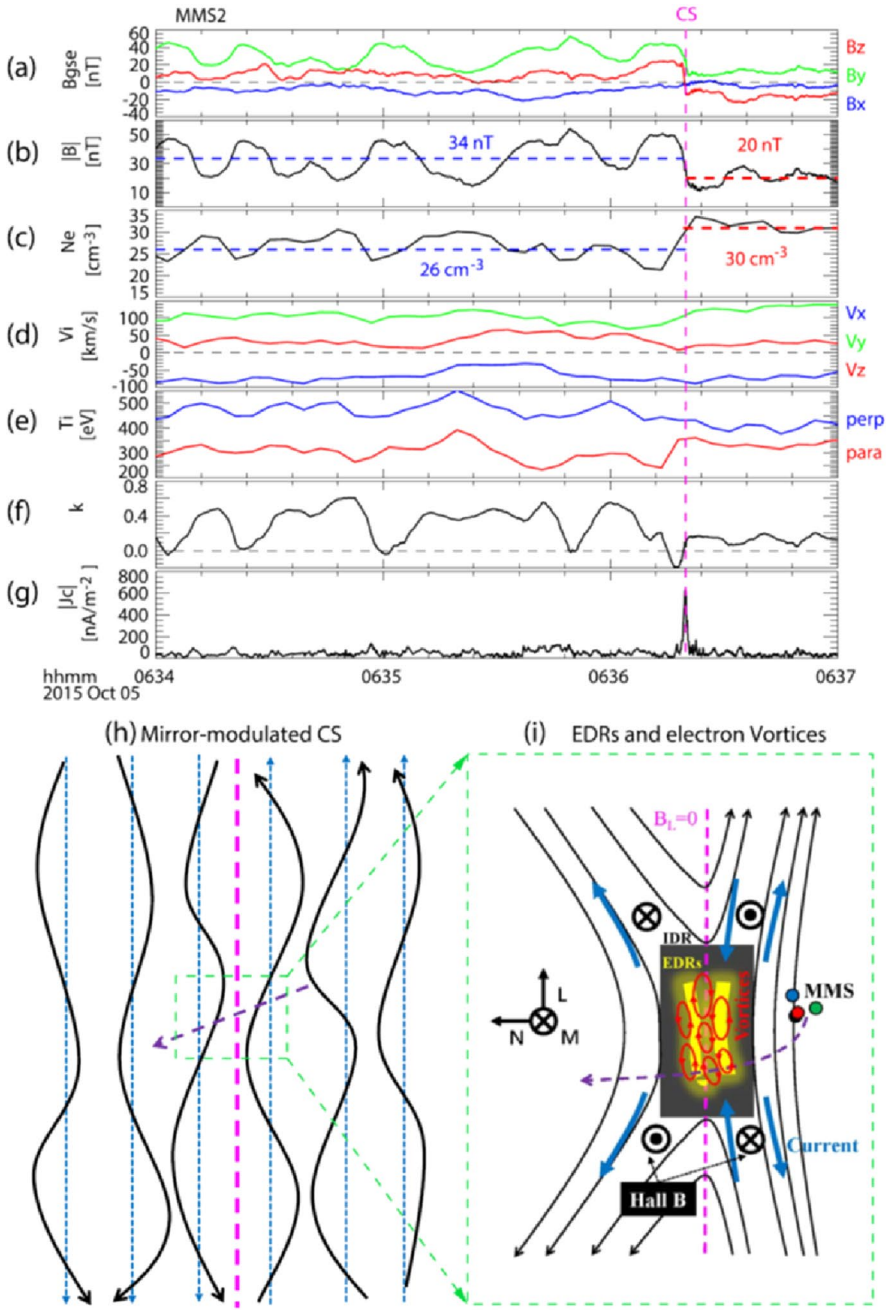

Fig. 4 Stacked EDR observed by MMS, adapted from Zhong et al. (2022). **a** Three components of the magnetic field; **b** total magnetic field; **c** electron density; **d** ion bulk velocities; **e** ion temperatures; **f** the parameter $k = \frac{T_{i\perp}}{Ti_{\parallel}} - \left(1 + \frac{1}{\beta_{\perp}}\right)$, which is critical to the ion-mirror instability; **g** current density estimated by the curlometer method, $J_c = \nabla \times B$. **h** A sketch of the mirror-modulated reconnecting current sheet. **i** A sketch of two EDRs and electron flow vortices (red rings) within the IDR

and electron K–H instability are important in three-dimensional reconnection, since they can control the electron dynamics and structure of the diffusion region through cross-scale coupling.

The EDR is comprised of the inner and outer EDR (Shay et al. 2007; Phan et al. 2007; Karimabadi et al. 2007). The outer EDR can extend far downstream of the X-line, manifested as a super-Alfvénic electron jet (Goldmann et al. 2011; Le et al. 2013; Zhou et al. 2014b). It is found that the out-of-plane non-ideal electric field in the outer EDR is opposite to the reconnection electric field E_M in the inner EDR (Shay et al. 2007; Karimabadi et al. 2007). Thus, the energy dissipation $J \cdot E'$ in the outer EDR is negative, in contrast with the positive $J \cdot E'$ in the inner EDR (Hwang et al. 2017; Xiong et al. 2022). This feature is used to differentiate the inner and outer EDR. One another important difference is that the inner EDR may control the reconnection rate, while the outer EDR does not, since electron inflows do not go through the outer EDR (Karimabadi et al. 2007). Recently, Zhong et al. (2020b) report a long EDR that extended at least 20 ion inertial lengths downstream of an X-line at the Earth's magnetopause. This EDR was detected in the exhaust of an asymmetric reconnection with a moderate guide field, the reconnection rate of which was ~ 0.1. It corresponds to strong positive energy dissipation ($J \cdot E' > 0$) and enhancement of the electron non-gyrotropy. The energy dissipation was contributed by the electron jet and non-ideal electric field along the outflow direction, which suggests that the EDR probably plays a more important role in the energy conversion in reconnection than previously thought. Huang et al. (2021) reported a similar long-extension EDR in electron-only reconnection in an ion-scale current sheet at the magnetopause. These extended EDRs have not been found in previous observations and simulations, hence posing a new view of the structure of the EDR in the asymmetric reconnection, which deserves further investigation from both simulations and observations.

2.3 Waves in the diffusion region

A fruitful of waves have been detected in the diffusion region, from below the ion cyclotron frequency to above the electron plasma frequency. The reason that plasma waves attract much attention and deserve exploring is twofold. First, the excitation of waves is intimately related to plasma kinetics; hence, studying the wave activities will shed new light on the particle dynamics. Second, it is believed that plasma waves play certain roles in reconnection, such as providing anomalous effects necessary for reconnection or energizing particles. Below we will review some of the most intensively investigated waves in the diffusion region.

It is suggested that kinetic Alfven wave (KAW) contributes to transporting energy away from the reconnection site (Chaston et al. 2005, 2009; Shay et al. 2011; Liang et al. 2016) via the Poynting flux and efficient heating of ions in both the perpendicular and parallel directions to the magnetic field, and heating of electrons parallel to the magnetic field. The Hall electromagnetic structures in the diffusion region are suggested as the signatures of KAWs propagating outward along the separatrix regions (Rogers et al. 2001; Dai 2009, 2018; Shay et al. 2011; Zhang et al. 2017;

Huang et al. 2018a). Furthermore, it is also found that the dominant wave mode in turbulence driven by reconnection is the fast whistler-mode or Alfven-whistler wave (Huang et al. 2010, 2012a, b). Huang et al. (2012a, b) estimated the electric field provided by anomalous resistivity caused by the kinetic Alfven turbulence, which is about 3 mV/m, close to the typical reconnection electric field in the magnetotail.

Because of the strong density gradient across the current sheet, the lower hybrid drift wave (LHDW) is readily be excited in the current sheet by the diamagnetic drift (e.g., Davidson et al. 1977). LHDW has long been regarded as one of the most important waves in contributing to anomalous transport (e.g., Silin et al. 2005). The fastest growing LHDW was observed to be confined at the edge of the reconnecting current sheet (Bale et al. 2002; Zhou et al. 2009a, 2014a, 2018a). This fastest growing mode is electrostatic with a typical wavelength of $k\rho_e \sim 1$ (ρ_e is the electron gyro-radius) and is heavily damped in regions where plasma β is high, such as the central current sheet. However, this electrostatic LHDW can survive in the central IDR in the presence of a large guide field, which greatly reduces the plasma β (Zhou et al. 2018a). On the other hand, longer wavelength electromagnetic mode LHDW can penetrate into the central current sheet and may significantly modify the reconnection process (Daughton et al. 2004; Zhou et al. 2009a), such as providing anomalous resistivity to support the reconnection electric field (Ji et al. 2004, 2005) and resulting in current sheet kinking (Cozzani et al. 2021). Graham et al. (2017b) found that the LHDW can heat the cold magnetospheric ions and produce cross-field particle diffusion, enabling magnetosheath electrons to enter the magnetospheric inflow region, thereby broadening the density gradient in the IDR, but not likely to produce anomalous fields. Recently, Chen et al. (2020) reported the LHDW driving electron heating and vortical flows in an electron-scale reconnection layer with a guide field. Electrons accelerated by the electrostatic potential of the waves exhibit perpendicular and non-gyrotropic heating.

Whistler waves have been suggested as the key mechanism to mediate fast reconnection (Mandt et al. 1994; Deng and Mastumoto 2001; Khotyaintsev et al. 2004). Whistler waves have frequently been detected in the ion diffusion region, particularly at the separatrix region (Khotyaintsev et al. 2020; Zhou et al. 2011a, 2018a; Zhong et al. 2021b), at the flux pileup region (Fu et al. 2014; Khotyaintsev et al. 2011; Le Contel et al. 2009; Zhou et al. 2013) and inside the EDR (Tang et al. 2013; Cao et al. 2017). Whistler wave in the reconnection diffusion region is typically generated by electron beams, temperature anisotropy, or loss-cone type distributions (Khotyaintsev et al. 2019). Whistler waves generally have a wavelength comparable to the scales of the typical EDR extent. Thus, whistlers may provide anomalous effects for reconnection. For example, Burch et al. (2018) show an intense energy dissipation driven by a highly oblique electrostatic whistler wave in the EDR. However, Zhong et al. (2022) show that electromagnetic whistlers, which propagate into the EDR from separatrix, did not provide sufficiently large anomalous dissipation in this EDR. Whether whistlers can provide sufficient anomalous effects in the EDR is still an open question.

Large-amplitude electrostatic waves have also been widely observed in the diffusion region, such as the Langmuir wave (Deng 2004; Zhou et al. 2016a), upper hybrid wave (Graham et al. 2017a), electron Bernstein wave (Li et al. 2020) and

broadband $E_{||}$ waves (Deng 2004; Cattell 2005; Graham et al. 2017a, b). They are generated by deformations in the electron VDF, such as the crescent-type electron VDF, electron beam, ring, shell, or loss-cone distributions (Khotyaintsev et al. 2019). These large-amplitude electrostatic waves can be observed in/near the EDR. Figure 5 shows an example of electron Bernstein wave driven by the perpendicular electron crescent-type VDF observed near the EDR (Li et al. 2020).

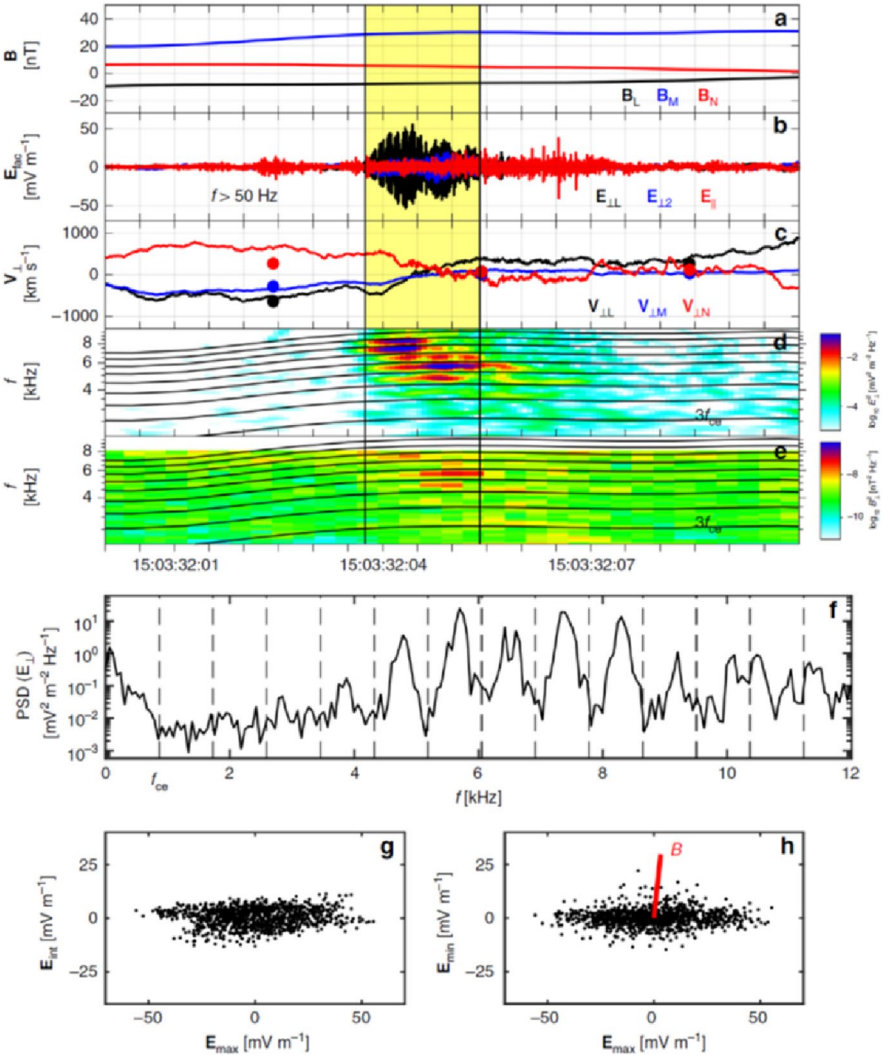

Fig. 5 Electron Bernstein waves observed near EDR, adapted from Li et al. (2020). **a** Magnetic fields. **b** Perpendicular and parallel components of the high-frequency E with $f > 50$ Hz. **c** $E \times B/B^2$ (lines) and 30-ms resolution $V_{e,\perp}$(dots). **d** Power spectrogram of $E_\perp$. **e** Power spectrogram of B. The electron cyclotron harmonic frequencies are plotted in (**d**, **e**). **g** and **h** Hodograms of E_{max} versus E_{int}, and E_{max} versus E_{min}. The red line in (**h**) denotes the B direction

Because of the large amplitude, these electrostatic waves may be able to thermalize and diffuse electrons in the diffusion region (Khotyaintsev et al. 2020). However, there is a lack of quantitative estimates of anomalous effects, cross-field diffusion or momentum transfer caused by these large-amplitude electrostatic waves in reconnection.

3 Outflow region

In the outflow region (some literatures use the term "exhaust" to indicate the same region), fast plasma flows carrying reconnected magnetic flux leaves the diffusion region. It is recently realized that the outflow region is a significant region where a large fraction of magnetic energy is dissipated (e.g., Angelopoulos et al. 2013; Zhou et al. 2021). Since its area is much larger than the diffusion region, it may contribute more to the energy dissipation than the diffusion region. Kinetic physics is important in this region and plays key role in regulating the energy conversion in the outflow.

3.1 Reconnection front

Energy conversion in the outflow region often occurs in coherent magnetic structures, one of which is the reconnection front (RF). RF is characterized by a rapid increase of the magnetic component normal to the current sheet (it is the B_z component in the magnetotail), and is usually followed immediately by a flux pileup region where magnetic flux is accumulated (Khotyaintsev et al. 2011; Fu et al. 2012). It is well known as the dipolarization front in the magnetotail, because the magnetic field becomes dipolarized associated with the dipolarization front (e.g., Nakamura et al. 2002; Runov et al. 2009; Zhou et al. 2009b; Deng et al. 2010), and jet front, since it is the leading edge of the fast reconnection outflow (e.g., Khotyaintsev et al. 2011). Dipolarizing flux bundle is also used to describe the RF and the flux pileup region together (e.g., Liu et al. 2013a). RF is a boundary layer that separates the ambient cold plasma from the hot tenuous plasma from reconnection (Runov et al. 2011). It is also deemed as the leading edge of the plasma depleted flux tube, i.e., plasma bubble, which is an entropy-depleted flux tube with a small dawn-dusk cross-section (e.g., Birn et al. 2004). Interestingly, the trailing edge of the plasma bubble is also a sharp boundary layer with a rapid decrease of magnetic field B_z (Zhou et al. 2013). Note that RF is also observed in tailward flow in the magnetotail, resembling a mirror image of the RF in the earthward flows (Zhou et al. 2011b; Li et al. 2014).

The formation of the RF is intrinsically related to reconnection. There are several mechanisms proposed to explain the formation of the RF: a product of transient magnetic reconnection (Sitnov et al. 2009; Fu et al. 2013; Zhou et al. 2011b); the interaction between the fast flow and ambient plasma, destabilizing the interchange or ballooning instability, the nonlinear evolution of which may produce the RF in the plasma sheet (Pritchett et al. 2014); erosion of the leading edge of the flux rope, which causes a noticeable asymmetric bipolar B_z across the MFR (Lu et al. 2015;

Fig. 6 Electromagnetic energy conversion at RFs, adapted from Angelopoulos et al. (2013). **a** X–Z satellite projections and a sketch of the magnetotail configuration on 3 July 2012, 09:40 UT, obtained by modifying the T96 model field. **b** and **c** Eight-minute detail of flux transport per unit of Y distance and energy conversion per unit Y–Z area observed past P2 and P3 after the second intensification. Red and blue in (**c**) are the cumulative power conversion due to the measured electric field or the MHD approximation. **d** Detail (25-s) of E_y, B_z during front passage by P2. **e** Tailward-moving power conversion density J_yE_y at P2 in the MHD approximation (blue) and using the measured E_y (red); **f** and **g** Detail of the same quantities at P3, as in (**d** and **e**), for P2

Man et al. 2018; Poh et al. 2019). It is also shown that RF can be generated by asymmetric reconnection, both in kinetic simulation (Song et al. 2019) and observed at magnetopause (Genestreti et al. 2020).

RF is generally an ion-scale current sheet with both intense transverse and field-aligned current (e.g., Huang et al. 2012b). The field-aligned current may connect to the ionosphere, which is important for ionosphere–magnetosphere coupling. It is suggested that a collapsing dipolarizing flux bundle could be an elemental substorm current wedge that can divert a sizable portion of the cross-tail current into the auroral ionosphere (Liu et al. 2013a).

RF is an important site for continuous energy conversion from electromagnetic fields to plasmas. Angelopoulos et al. (2013) found that RF in the magnetotail can account for nearly the overall global magnetic flux reduction during a magnetospheric substorm. They also found that the intense energy conversion at the RF predominantly occurs within electron scale (~ 1–10 electron inertial lengths) intense current sheets in the RF (Fig. 6). A statistical study using cluster multi-spacecraft measurements confirms that RF is indeed a load region in the magnetotail (Huang et al. 2012b, 2015a). Electron-scale sub-structures have been identified at RF recently by MMS observations (Liu et al. 2018a, b; Zhou et al. 2019a). Although DF is primarily an energy-load region ($E{\cdot}J>0$), the electron-scale currents could lead to a localized energy generation ($E{\cdot}J<0$). This suggests that the current, electric field and energy conversion are not uniform across the RF (Liu et al. 2018a, b).

Energetic particles have frequently been detected around the RF (Zhou et al. 2009b; Fu et al. 2011). The energization mechanism of high-energy particles by RF has been intensively studied in the past decade. Using THEMIS observations and test particle simulation, Zhou et al. (2010) find that ions in the ambient plasma are reflected and accelerated by the approaching front. Recently, it is found RFs with rippled structures are more efficient in accelerating ions than those without surface ripples (Bai et al. 2022). Ions can be trapped at the front layer due to the large magnetic gradient, since the large gradient drift turns the ions around, precluding them from leaving the fast flows (Ukhorskiy et al. 2018).

Ions are mostly non-adiabatic around the RF, because their Larmor radii are typically larger than the gradient scale around the RF. On the other hand, electrons are mostly adiabatically accelerated at RF because of their much smaller gyro-radii. Ashour-Abdalla et al. (2011) combined a global MHD simulation and test particle simulation to investigate the electron acceleration in the magnetotail. One main conclusion is that the energetic electrons in the magnetotail are not produced by local reconnection, but are produced by earthward moving RF through adiabatic

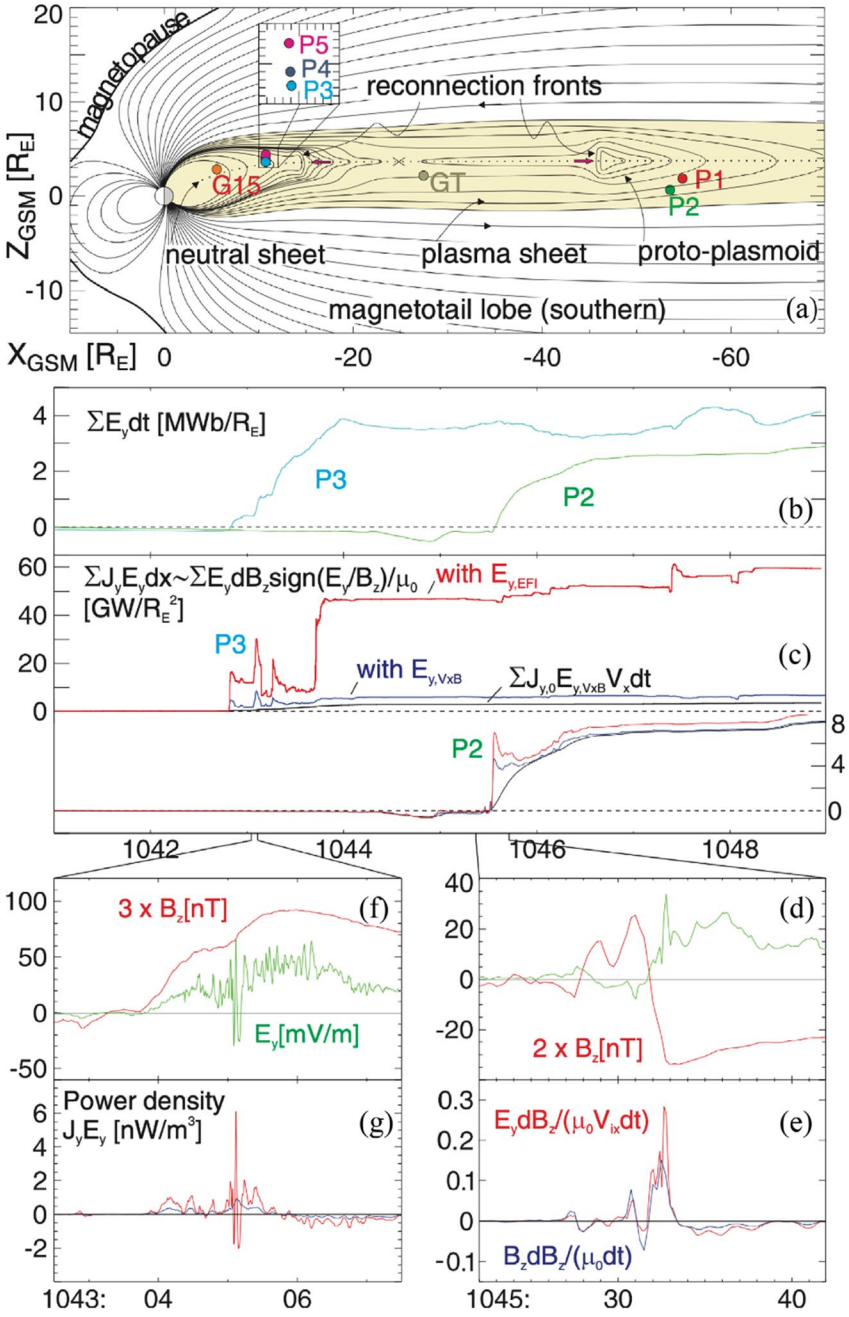

acceleration. Fu et al. (2011, 2013) employed the Liouville mapping method to identify and quantify the adiabatic acceleration of electrons at and behind the RF. They suggest that betatron and Fermi acceleration are responsible for the energetic

electron fluxes enhancement associated with RFs. The presence of parallel electric field at the RF could trap the electrons along the field line and facilitate more efficient electron acceleration at the RF (Huang et al. 2015b). Different types of electron pitch angle distributions are observed at/near the RF: pancake distribution (the highest flux at 90°), cigar-type distribution (highest flux at 0° and 180°), and rolling-pin distribution (the highest flux at 0°, 90° and 180°). The pancake and cigar-type distribution are mainly caused by betatron and Fermi acceleration, respectively, while the rolling-pin distribution is probably results from the combined process of a local-scale betatron and a global-scale Fermi acceleration (Liu et al. 2017).

Strong gradient in magnetic fields and plasma can drive plasma instability unstable at the RF. For example, large-amplitude LHDWs have been observed at the front layer, where the strong diamagnetic drift provides the free energy source (e.g., Zhou et al. 2009b). In addition, non-Maxwellian distribution formed at/around the RF supplies the free energy for the waves. Various kinds of plasma waves have been detected at/around the RF, such as magnetosonic waves (ion Bernstein wave), LHDWs, whistler waves, electron cyclotron harmonic waves and electrostatic solitary structures (Zhou et al. 2009b, 2014c; Deng et al. 2010; Fu et al. 2014; Li et al. 2014; Huang et al. 2012b; Khotyaintsev et al. 2011; Liu et al. 2022). These waves may lead to particle acceleration and pitch angle scattering at/around the RF. For instance, using quasi-linear calculation, Zhou et al. (2014c) find that large-amplitude magnetosonic waves can accelerate electrons to very high energy in a few tens seconds. Liu et al. (2022) present the MMS observations of electrostatic solitary waves at the RF in the magnetotail. The excitation of the solitary waves will reduce the field-aligned current, and thus, the micro-scale physics driven by large-scale dynamics finally reacts on the large-scale magnetosphere–ionosphere coupling.

3.2 Magnetic flux rope

Another common and critical coherent structure in the outflow region is the magnetic flux rope (MFR). MFRs with different spatial sizes, ranging from tens of R_E to a few ion inertial lengths, have been observed in the fast outflow (Slavin et al. 2003; Zhong et al. 2020a). Magnetic field lines with different connectivity were observed in one FTE at the dayside magnetopause. The electron energy-pitch angle distribution implies that the FTE was composed of flux ropes of all four possible magnetic topologies, indicating an intrinsic property of FTEs formed by 3D multiple X-line reconnection distinguished from quasi 2D FTE models (Pu et al. 2013). The internal structure of small-scale MFRs is also quite complex. Wang et al. (2010) found distinct features between the outer and core regions of a secondary MFR inside an IDR. The core region is characterized by a plasma density dip, strong core field and weak wave activity, while the outer region is characterized by relatively high plasma density and strong wave activity. The field-aligned current mainly carried by electron beams in the outer region produced the strong out-of-plane core field inside the MFR. Recent MMS observations show that the rapid variations of electron density are correlated with the changes in electron temperature and pitch angle anisotropy inside an ion-scale MFR (Man et al. 2020). They suggest that the coexistence of

different magnetic field line topologies inside the secondary MFR is responsible for the observed electron pitch angle distributions.

One important MFR dynamics is the coalescence between MFRs. This phenomenon has been studied mainly in simulation and theory for many years, whereas in situ observation of coalescence is rare. Recent high-resolution data from Cluster and MMS unraveled the dynamics of flux rope coalescence in space plasma. Wang et al. (2016) reported a series coalescence between ion-scale MFRs in an IDR, while Zhou et al. (2017) reported the coalescence between two macroscopic flux ropes, with spatial size up to 100 ion inertial lengths, in a reconnection outflow far from the X-line. They also identified the EDR of the reconnection between the two MFRs. Moreover, suprathermal electrons were detected in this EDR, suggesting that coalescence can be an efficient engine for electron acceleration.

MFRs not only coalesce with each other, and they can also merge with ambient field lines when there is a large angle between the magnetic field lines in the flux rope and in the ambient plasma. For example, in the magnetotail, the earthward propagating flux rope can reconnect with the geomagnetic field (Man et al. 2018, 2020; Poh et al. 2019), which can consume the magnetic flux in the flux rope and may lead to the formation of the dipolarization front (Lu et al. 2015). Another example is the electron-scale reconnection between the magnetopause MFR and the Hall out-of-plane magnetic field (Zhong et al. 2021a). This reconnection is special, because the reconnecting magnetic component is the core field of the MFR, which points in the out-of-plane direction of the primary reconnection. Hence, this secondary reconnection in the outflow of the primary reconnection is essentially a 3D reconnection. It converts the magnetic energy into heating plasma, which leads to a cross-scale energy conversion for reconnection: magnetic reconnection produces ion-scale flux ropes which store a significant amount of magnetic energy mainly in its core component. The electron-scale reconnection between the ion-scale flux rope and the ambient magnetic field finally dissipates the energy to heat plasma. Magnetic reconnection also occurs inside the MFR. Øieroset et al. (2016) report reconnection at the center of a large-scale flux rope. The reconnecting current sheet was compressed by the colliding reconnection jets. Wang et al. (2020) reveal electron-scale reconnection in current filaments inside a couple of ion-scale MRF. These electron-scale reconnections lead to energy dissipation within the ion-scale MFRs, also a good example of cross-scale energy dissipation during reconnection. We should note that the magnetic energy can be dissipated within the MFR even without local reconnection or coalescence (Huang et al. 2019).

MFR is an important structure for energizing particles to high energy (Drake et al. 2006; Fu et al. 2006; Zhou et al. 2018b; Zhong et al. 2020a). It is proposed that the contracted MFR can efficiently accelerate electrons through the first-order Fermi acceleration. Moreover, particles can be accelerated during MFR coalescence, either by the reconnection electric field at the merging line (Oka et al. 2010a) or by the Fermi mechanism due to the shrink of the field lines during coalescence (Drake et al. 2013). Oka et al. (2010b) also propose an island-surfing scenario that electrons can be trapped inside the secondary island and energized by the reconnection electric field when the island is inside the diffusion region. Satellite observations have established a close relationship between high-energy electrons and MFR. In

particular, Zhong et al. (2020a) quantify the electron acceleration rate from betatron, Fermi mechanisms and by the parallel electric field using the formula derived in Dahlin et al. (2014). They find that the most energetic electrons were energized by betatron acceleration at the center of the MFR (Fig. 7). Although Fermi acceleration rate is comparable to the rate of betatron acceleration, field-aligned electrons can easily escape from the MFR along the axis of the rope.

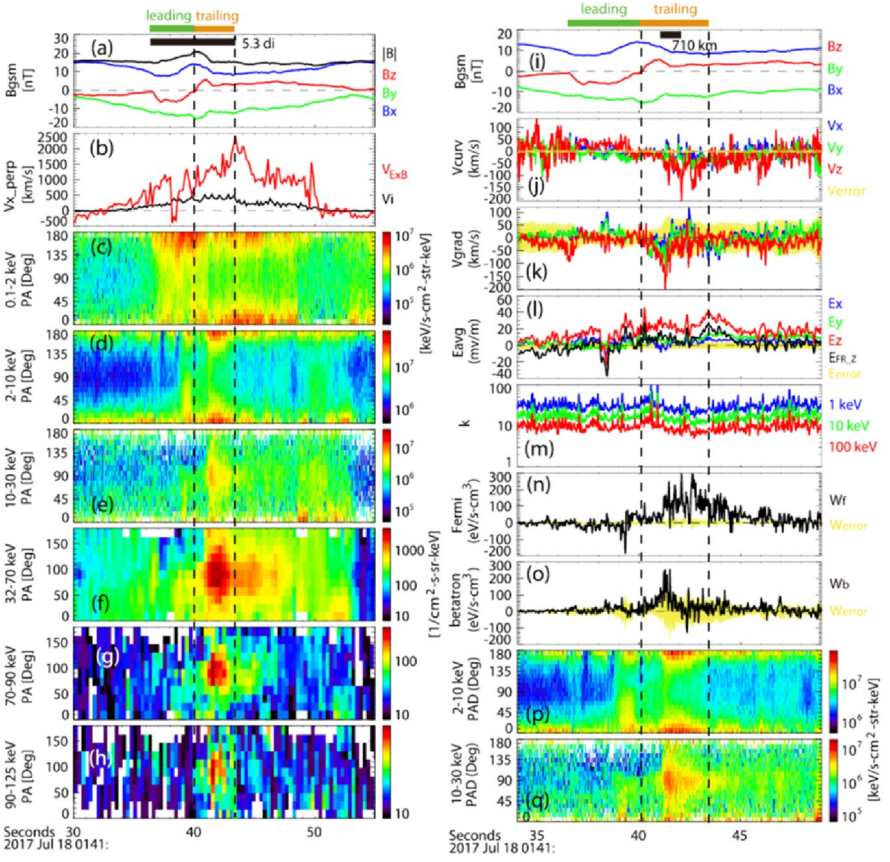

Fig. 7 Electron pitch angle distribution (PAD) and electron local acceleration rate within the MFR, adapted from Zhong et al. (2020a). Panel **a** shows three components and magnitude of the magnetic fields; **b** earthward perpendicular ion bulk velocity V_i and V_{ExB}; **c**–**h** electron PAD in different energy ranges; **i** three components of magnetic fields observed by MMS2, **j** curvature drift, and **k** gradient drift velocity of electrons and their uncertainties (yellow); **l** three components of electric fields and the Z component of the electric field in the FR frame $(E+V_{FR}\times B)_Z$ (black); **m** the value of k which is the square root of the ratio between the magnetic field curvature radius and the particle's Larmor radius; **n** the bulk energy gains of electrons from local Fermi acceleration and **o** local betatron acceleration and their uncertainties (yellow); and **p** 2–10 and **q** 10–30 keV electrons PAD observed by MMS2

3.3 Other coherent structures

Besides RF and MFR, there are other electron-scale structures within the outflow region. Vertical electron-scale current sheets have been detected inside the outflow (Zhou et al. 2019a, 2021). Some of these current sheets are not related to either MFRs or RF, and are likely a consequence of turbulent evolution of the fast flows. Figure 8 illustrates many current filaments in a turbulent outflow (Zhou et al. 2021). Electron-only reconnection was detected within these thin current sheets. It is suggested that these secondary reconnections in the fast flows contribute significantly to the overall energy release during the primary reconnection.

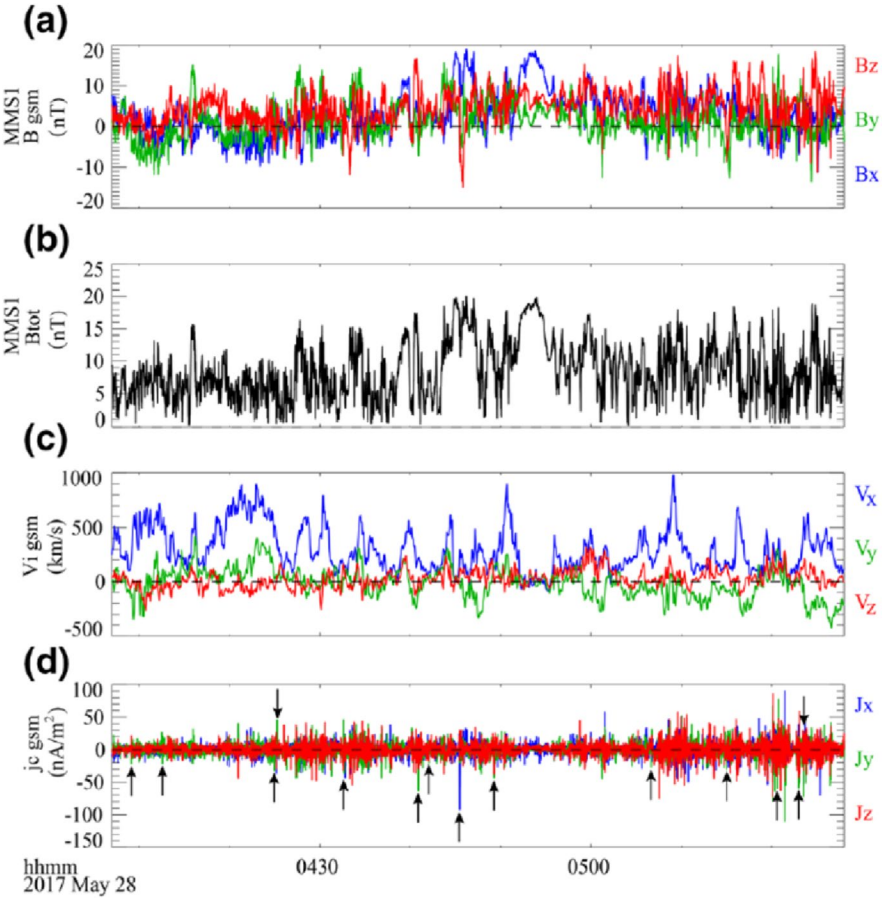

Fig. 8 MMS observations of the turbulent outflow and secondary reconnections in the magnetotail (adapted from Zhou et al. 2021). **a** Three components of the magnetic field; **b** total magnetic fields; **c** ion bulk flow; **d** electric current density calculated by the curlometer technique based on the four spacecraft data. The black arrows in panel (**d**) mark the current filaments which were reconnecting

4 Separatrix region

The separatrix region is a kinetic-scale boundary layer that separates the reconnected field lines and un-reconnected field lines (e.g., Vaivads 2004). We can also treat it as the boundary between the inflow and outflow region in reconnection. It originates from the diffusion region and extends far away from the X-line, connecting the micro-scale diffusion region to the macro-scale boundary. Therefore, one can expect that the physical processes inside the diffusion region can be monitored at a distance, e.g., by monitoring parallel electron beams emanating from the X-line. On the other hand, it is also interesting to know how does the separatrix region interact with boundaries such as ionosphere (Vaivads et al. 2004).

Electron inflows are almost along the separatrix into the EDR at the inflow side, while electron outflows are away from the reconnection site at the outflow side of the separatrix. Electron mainly carries the current around the separatrix region, forming a current loop, which gives rise to the out-of-plane quadrupolar magnetic fields. Density depletion layer or density cavity is formed at the separatrix region due to the requirement to maintain the pressure balance at the separatrix because of the enhancement of the magnetic field (Shay et al. 2001). The density cavity has a quadrupolar distribution along the four arms of the separatrix without guide field. While the guide field alters the structure as the density cavity appears only in two arms of the separatrix while the density increases at the other two arms of the separatrix. Figure 9 shows a 2D particle-in-cell simulation of the density cavity formed along the separatrix in guide field reconnection (Zhou et al. 2011a). One can see that the two arms with density cavity correspond to the enhancement of the out-of-plane magnetic field, the polarity of which is the same as the guide field.

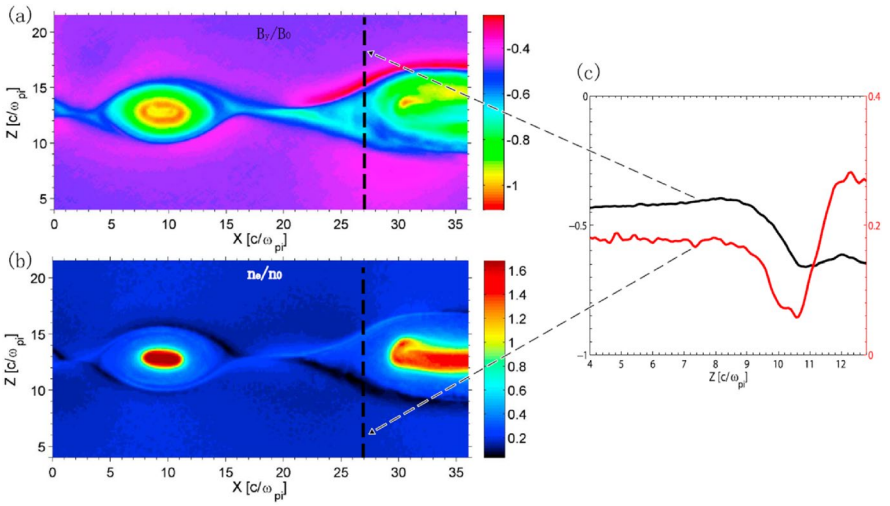

Fig. 9 PIC simulation of density cavity formed at the separatrix region, adapted from Zhou et al. (2011a)

Recent MMS observations show that the separatrix region is more turbulent and dynamic than previous thought. For example, there exist filamentary currents with large current density at the separatrix region (Phan et al. 2016) and large-amplitude non-ideal electric field, which leads to intense oscillating energy dissipation (Yu et al. 2019; Zhou et al. 2019a). Electron beams are frequently observed in the separatrix region. In addition, loss-cone distributions are another type of typical VDFs observed in the separatrix region of magnetopause reconnection where the plasma properties at the two sides of the current sheet are distinct (Khotyaintsev et al. 2019). Whistler waves in separatrix regions are likely driven by electron beams via Landau resonance (Zhou et al. 2011a; Fujimoto 2014; Ren et al. 2019) or loss-cone distribution via cyclotron resonance (Graham et al. 2016; Zhong et al. 2021b). Whistlers generated by cyclotron resonance propagate quasi-parallel to the ambient magnetic field, while whistlers generated by Landau resonance propagate quasi-oblique to the magnetic field. Lower hybrid waves were also frequently detected at the separatrix as the density gradient at the separatrix region gives rise to diamagnetic drift which drives lower hybrid drift waves (Retino et al. 2006; Graham et al. 2017b; Ergun et al. 2017). Electron beam is also a possible free energy source for lower hybrid waves at the separatrix region (Zhou et al. 2011a). These lower hybrid waves can heat electrons via Landau resonance as revealed by simulations (Le et al. 2017, 2018) and in situ observations (Graham et al. 2017b). The lower hybrid waves observed on the magnetopause may also be important for plasma diffusion by providing large anomalous diffusion rate (Silin et al. 2005). ESWs or electron holes have been detected at the separatrix region (Cattell 2005). Buneman instability or electron–electron instability (e.g., bump-on-tail instability) is probably responsible for the ESWs. Interestingly, ESWs with distinct propagation speeds were observed at the separatrix region of asymmetric reconnection at the dayside magnetopause, suggesting that multiple instabilities are occurring (Graham et al. 2015).

5 Summary and outlook

This paper provides a review of kinetic physics associated with magnetic reconnection based primarily on recent magnetospheric satellite observations. Here, we decompose the reconnection region into different sub-regions: the diffusion region, the outflow region and the separatrix region, which is the boundary between the inflow and outflow region. Then, we review the recent progress in understanding the kinetic processes occurring in these different regions, though the coupling among different regions is less intensively studied and unclear. The cross-region and cross-scale couplings are the most rewarding and challenging research topics in the future.

It is worth noting that kinetic physics also plays certain roles in the inflow region, where electrons are anisotropy with parallel temperature larger than perpendicular temperature. The cause of this anisotropy has been well documented by Egedal et al. (2013), which suggests that the anisotropy is essentially caused by particle trapping and strong parallel electric fields develop in conjunction with this anisotropy. The parallel electric fields can be important for electron acceleration.

There are following open questions we would like to bring to attention for the community.

(A) Onset problem. Reconnection does not always proceed at a constant speed, for say, ~ 0.1. Thus, there must be a magnetic energy storage phase before the onset of reconnection. A typical example is the Earth's magnetotail, where magnetic energy is accumulated before the rapid release by reconnection. One controversial issue is whether the macro-physics at the boundary layer or micro-physics in the diffusion region determines the onset of reconnection. This is illustrated as the outside (boundary) versus inside (diffusion region) problem (Hesse and Cassak 2020). Moreover, it is important to figure out the exact physical process triggering reconnection.

Since space plasma is collisionless, anomalous resistivity has long been invoked to provide the necessary non-ideal effect to break field lines in the diffusion region and possibly initiate reconnection (Treumann 2001). Recent 3D full particle simulations show that anomalous terms (anomalous drag or viscosity) could provide the necessary electric field for reconnection (Drake et al. 2003; Che et al. 2011; Fujimoto and Sydora 2012; Price et al. 2016); however, the observational evidence for anomalous resistivity to support the reconnection electric field is missing (Mozer et al. 2011).

Another controversial issue related to the onset problem is whether ion physics (Schindler 1974; Sitnov and Schindler 2010) or electron physics (Coppi et al. 1966) determine the onset. This is equivalent to contrasting the role of ion-tearing mode and electron-tearing mode in triggering reconnection. Recently, by combining PIC simulation and MMS observation, Lu et al. (2020) illustrate that magnetotail reconnection starts from electron reconnection in the presence of a strong external driver, which is an important step toward solving this problem.

(B) Reconnection and turbulence. Reconnection and turbulence are two intertwined energy dissipation processes in space and astrophysical plasma. It has been shown that reconnection occurs in coherent structures spontaneously formed in turbulence, and reconnection also drives turbulence that may have significant feedback on reconnection (Lapenta 2008; Ergun et al. 2018; Jin et al. 2022). One of the most critical questions in turbulence is how does the energy dissipate in the dissipation range (e.g., Retinò 2016). Recently, it is found that the reconnection in turbulence may play important roles in terminating the energy cascade in the inertial range in turbulence (Retino et al. 2007; Sundkvist et al. 2007; Phan et al. 2018).

On the other hand, the effect of turbulence on reconnection is largely unknown. 3D PIC simulations show that the 3D evolution of the reconnection layer is distinct from that in 2D in that multiple oblique tearing resonance layer exists and produces many more MFRs than 2D (Daughton et al. 2011; Liu et al. 2013b). This means that 3D reconnection is more turbulent than 2D. However, the reconnection rate and energy conversion are not obviously different than 2D. The feedback of reconnection-driven turbulence on reconnection needs to be further investigated observationally, especially, the effect of turbulence on the key parameters of reconnection.

(C) How does the kinetic-scale physics affect the macroscopic topology change and energy conversion (particle acceleration)? This is essentially related to the question of how does the physical processes in different scales couple in reconnection.

Addressing this question may require well-designed multiple spacecraft mission that can make simultaneous measurements at multiple scales and is capable of resolving cross-scale plasma processes ranging from kinetic scale to macro-scale, such as the recent proposed AME (self-Adaptive Magnetic reconnection Explorer) mission consisting of a cross-scale constellation of 12 + CubeSats and one mother satellite (Dai et al. 2020), or taking advantage of the pre-existing mission, for example, if properly arranged, MMS with spacing on the electron scale, cluster with spacing on the ion scale and THEMIS/ARTEMIS with spacing on the MHD (fluid) scale together could probably provide simultaneously observation at multiple scales.

Acknowledgements This work was supported by the National Natural Science Foundation of China (NSFC) under Grant No. 42104156, 42130211, 42074197, 41774154, and the project funded by China Postdoctoral Science Foundation under Grant No. 2021M691395.

Declarations

Conflict of interest On behalf of all authors, the corresponding author states that there is no conflict of interest.

References

V. Angelopoulos, W. Baumjohann, C.F. Kennel, F.V. Coroniti, M.G. Kivelson, R. Pellat et al., Bursty bulk flows in the inner central plasma sheet. J. Geophys. Res. **97**(A4), 4027 (1992). https://doi.org/10.1029/91JA02701

V. Angelopoulos, C.F. Kennel, F.V. Coroniti, R. Pellat, M.G. Kivelson, R.J. Walker et al., Statistical characteristics of bursty bulk flow events. J. Geophys. Res. **99**(A11), 21257 (1994). https://doi.org/10.1029/94JA01263

V. Angelopoulos, J.P. McFadden, D. Larson, C.W. Carlson, S.B. Mende, H. Frey et al., Tail reconnection triggering substorm onset. Science **321**(5891), 931–935 (2008). https://doi.org/10.1126/science.1160495

V. Angelopoulos, A. Runov, X.-Z. Zhou, D.L. Turner, S.A. Kiehas, S.-S. Li, I. Shinohara, Electromagnetic energy conversion at reconnection fronts. Science **341**(6153), 1478–1482 (2013). https://doi.org/10.1126/science.1236992

M. Ashour-Abdalla, M. El-Alaoui, M.L. Goldstein, M. Zhou, D. Schriver, R. Richard et al., Observations and simulations of non-local acceleration of electrons in magnetotail magnetic reconnection events. Nat. Phys. **7**(4), 360–365 (2011). https://doi.org/10.1038/nphys1903

K. Bai, Y. Yu, H. Huang, J. Cao, Simulating the ion-trapping acceleration at rippled reconnection fronts. Astrophys. J. **925**(1), 26 (2022). https://doi.org/10.3847/1538-4357/ac3a08

S.D. Bale, F.S. Mozer, T. Phan, Observation of lower hybrid drift instability in the diffusion region at a reconnecting magnetopause: LHDI at reconnecting magnetopause. Geophys. Res. Lett. **29**(24), 33-1-33–4 (2002). https://doi.org/10.1029/2002GL016113

N. Bessho, A. Bhattacharjee, Collisionless reconnection in an electron-positron plasma. Phys. Rev. Lett. **95**(24), 245001 (2005). https://doi.org/10.1103/PhysRevLett.95.245001

J. Birn, J.F. Drake, M.A. Shay, B.N. Rogers, R.E. Denton, M. Hesse et al., Geospace environmental modeling (GEM) magnetic reconnection challenge. J. Geophys. Res. Space Phys. **106**(A3), 3715–3719 (2001). https://doi.org/10.1029/1999JA900449

J. Birn, M.F. Thomsen, M. Hesse, Electron acceleration in the dynamic magnetotail: test particle orbits in three-dimensional magnetohydrodynamic simulation fields. Phys. Plasmas **11**(5), 1825–1833 (2004). https://doi.org/10.1063/1.1704641

D. Biskamp, Magnetic reconnection via current sheets. Phys. Fluids (1986). https://doi.org/10.1063/1.865670

A.L. Borg, M. Øieroset, T.D. Phan, F.S. Mozer, A. Pedersen, C. Mouikis et al., Cluster encounter of a magnetic reconnection diffusion region in the near-Earth magnetotail on September 19, 2003: cluster reconnection region crossing 19 Sept 2003. Geophys. Res. Lett. (2005). https://doi.org/10.1029/2005GL023794

J.L. Burch, R.B. Torbert, T.D. Phan, L.-J. Chen, T.E. Moore, R.E. Ergun et al., Electron-scale measurements of magnetic reconnection in space. Science **352**(6290), aaf2939 (2016). https://doi.org/10.1126/science.aaf2939

J.L. Burch, R.E. Ergun, P.A. Cassak, J.M. Webster, R.B. Torbert, B.L. Giles et al., Localized oscillatory energy conversion in magnetopause reconnection. Geophys. Res. Lett. **45**(3), 1237–1245 (2018). https://doi.org/10.1002/2017GL076809

J.B. Cao, Y.D. Ma, G. Parks, H. Reme, I. Dandouras, R. Nakamura et al., Joint observations by cluster satellites of bursty bulk flows in the magnetotail. J. Geophys. Res. **111**(A4), A04206 (2006). https://doi.org/10.1029/2005JA011322

D. Cao, H.S. Fu, J.B. Cao, T.Y. Wang, D.B. Graham, Z.Z. Chen et al., MMS observations of whistler waves in electron diffusion region: whistlers in electron diffusion region. Geophys. Res. Lett. **44**(9), 3954–3962 (2017). https://doi.org/10.1002/2017GL072703

C. Cattell, Cluster observations of electron holes in association with magnetotail reconnection and comparison to simulations. J. Geophys. Res. **110**(A1), A01211 (2005). https://doi.org/10.1029/2004JA010519

C.C. Chaston, T.D. Phan, J.W. Bonnell, F.S. Mozer, M. Acuña, M.L. Goldstein et al., Drift-kinetic Alfvén waves observed near a reconnection X line in the earth's magnetopause. Phys. Rev. Lett. **95**(6), 065002 (2005). https://doi.org/10.1103/PhysRevLett.95.065002

C.C. Chaston, J.R. Johnson, M. Wilber, M. Acuna, M.L. Goldstein, H. Reme, Kinetic Alfvén wave turbulence and transport through a reconnection diffusion region. Phys. Rev. Lett. **102**(1), 015001 (2009). https://doi.org/10.1103/PhysRevLett.102.015001

H. Che, J.F. Drake, M. Swisdak, A current filamentation mechanism for breaking magnetic field lines during reconnection. Nature **474**(7350), 184–187 (2011). https://doi.org/10.1038/nature10091

L.-J. Chen, A. Bhattacharjee, P.A. Puhl-Quinn, H. Yang, N. Bessho, S. Imada et al., Observation of energetic electrons within magnetic islands. Nat. Phys. **4**(1), 19–23 (2008). https://doi.org/10.1038/nphys777

L.-J. Chen, S. Wang, O. Le Contel, A. Rager, M. Hesse, J. Drake et al., Lower-hybrid drift waves driving electron nongyrotropic heating and vortical flows in a magnetic reconnection layer. Phys. Rev. Lett. **125**(2), 025103 (2020). https://doi.org/10.1103/PhysRevLett.125.025103

L. Comisso, M. Lingam, Y.-M. Huang, A. Bhattacharjee, Plasmoid instability in forming current sheets. Astrophys. J. **850**(2), 142 (2017). https://doi.org/10.3847/1538-4357/aa9789

B. Coppi, G. Laval, R. Pellat, Dynamics of the geomagnetic tail. Phys. Rev. Lett. **16**(26), 1207–1210 (1966). https://doi.org/10.1103/PhysRevLett.16.1207

G. Cozzani, Yu.V. Khotyaintsev, D.B. Graham, J. Egedal, M. André, A. Vaivads et al., Structure of a perturbed magnetic reconnection electron diffusion region in the earth's magnetotail. Phys. Rev. Lett. **127**(21), 215101 (2021). https://doi.org/10.1103/PhysRevLett.127.215101

J.T. Dahlin, J.F. Drake, M. Swisdak, The mechanisms of electron heating and acceleration during magnetic reconnection. Phys. Plasmas **21**(9), 092304 (2014). https://doi.org/10.1063/1.4894484

L. Dai, Collisionless magnetic reconnection via Alfvén eigenmodes. Phys. Rev. Lett. **102**(24), 245003 (2009). https://doi.org/10.1103/PhysRevLett.102.245003

L. Dai, Structures of hall fields in asymmetric magnetic reconnection. J. Geophys. Res. Space Phys. **123**(9), 7332–7341 (2018). https://doi.org/10.1029/2018JA025251

L. Dai, C. Wang, Z. Cai, W. Gonzalez, M. Hesse, P. Escoubet et al., AME: a cross-scale constellation of cubesats to explore magnetic reconnection in the solar-terrestrial relation. Front. Phys. **8**, 89 (2020). https://doi.org/10.3389/fphy.2020.00089

W. Daughton, G. Lapenta, P. Ricci, Nonlinear evolution of the lower-hybrid drift instability in a current sheet. Phys. Rev. Lett. **93**(10), 105004 (2004). https://doi.org/10.1103/PhysRevLett.93.105004

W. Daughton, J. Scudder, H. Karimabadi, Fully kinetic simulations of undriven magnetic reconnection with open boundary conditions. Phys. Plasmas **13**(7), 072101 (2006). https://doi.org/10.1063/1.2218817

W. Daughton, V. Roytershteyn, B.J. Albright, H. Karimabadi, L. Yin, K.J. Bowers, Transition from collisional to kinetic regimes in large-scale reconnection layers. Phys. Rev. Lett. **103**(6), 065004 (2009). https://doi.org/10.1103/PhysRevLett.103.065004

W. Daughton, V. Roytershteyn, H. Karimabadi, L. Yin, B.J. Albright, B. Bergen, K.J. Bowers, Role of electron physics in the development of turbulent magnetic reconnection in collisionless plasmas. Nat. Phys. **7**(7), 539–542 (2011). https://doi.org/10.1038/nphys1965

R.C. Davidson, N.T. Gladd, C.S. Wu, J.D. Huba, Effects of finite plasma beta on the lower-hybrid-drift instability. Phys. Fluids **20**(2), 301 (1977). https://doi.org/10.1063/1.861867

X.H. Deng, Geotail encounter with reconnection diffusion region in the Earth's magnetotail: evidence of multiple X lines collisionless reconnection? J. Geophys. Res. **109**(A5), A05206 (2004). https://doi.org/10.1029/2003JA010031

X.H. Deng, H. Matsumoto, Rapid magnetic reconnection in the Earth's magnetosphere mediated by whistler waves. Nature **410**(6828), 557–560 (2001). https://doi.org/10.1038/35069018

X. Deng, M. Ashour-Abdalla, M. Zhou, R. Walker, M. El-Alaoui, V. Angelopoulos et al., Wave and particle characteristics of earthward electron injections associated with dipolarization fronts: waves and particles during injections. J. Geophys. Res. Space Phys. (2010). https://doi.org/10.1029/2009JA015107

J.F. Drake, M. Swisdak, C. Cattell, M.A. Shay, B.N. Rogers, A. Zeiler, Formation of electron holes and particle energization during magnetic reconnection. Science **299**(5608), 873–877 (2003). https://doi.org/10.1126/science.1080333

J.F. Drake, M. Swisdak, K.M. Schoeffler, B.N. Rogers, S. Kobayashi, Formation of secondary islands during magnetic reconnection. Geophys. Res. Lett. **33**(13), L13105 (2006). https://doi.org/10.1029/2006GL025957

J.F. Drake, M.A. Shay, M. Swisdak, The Hall fields and fast magnetic reconnection. Phys. Plasmas **15**(4), 042306 (2008). https://doi.org/10.1063/1.2901194

J.F. Drake, M. Swisdak, R. Fermo, The power-law spectra of energetic particles during multi-island magnetic reconnection. Astrophys. J. Lett. **763**, L5 (2013)

J.W. Dungey, Interplanetary magnetic field and the auroral zones. Phys. Rev. Lett. **6**(2), 47–48 (1961). https://doi.org/10.1103/PhysRevLett.6.47

J.P. Eastwood, M.A. Shay, T.D. Phan, M. Øieroset, Asymmetry of the ion diffusion region hall electric and magnetic fields during guide field reconnection: observations and comparison with simulations. Phys. Rev. Lett. **104**(20), 205001 (2010). https://doi.org/10.1103/PhysRevLett.104.205001

J. Egedal, A. Le, W. Daughton, A review of pressure anisotropy caused by electron trapping in collisionless plasma, and its implications for magnetic reconnection. Phys. Plasmas **20**(6), 061201 (2013). https://doi.org/10.1063/1.4811092

J. Egedal, A. Le, W. Daughton, B. Wetherton, P.A. Cassak, L.-J. Chen et al., Spacecraft observations and analytic theory of crescent-shaped electron distributions in asymmetric magnetic reconnection. Phys. Rev. Lett. **117**(18), 185101 (2016). https://doi.org/10.1103/PhysRevLett.117.185101

J. Egedal, A. Le, W. Daughton, B. Wetherton, P.A. Cassak, J.L. Burch et al., Spacecraft observations of oblique electron beams breaking the frozen-in law during asymmetric reconnection. Phys. Rev. Lett. **120**(5), 055101 (2018). https://doi.org/10.1103/PhysRevLett.120.055101

R.E. Ergun, L.-J. Chen, F.D. Wilder, N. Ahmadi, S. Eriksson, M.E. Usanova et al., Drift waves, intense parallel electric fields, and turbulence associated with asymmetric magnetic reconnection at the magnetopause: waves and turbulence in reconnection. Geophys. Res. Lett. **44**(7), 2978–2986 (2017). https://doi.org/10.1002/2016GL072493

R.E. Ergun, K.A. Goodrich, F.D. Wilder, N. Ahmadi, J.C. Holmes, S. Eriksson et al., Magnetic reconnection, turbulence, and particle acceleration: observations in the earth's magnetotail. Geophys. Res. Lett. **45**(8), 3338–3347 (2018). https://doi.org/10.1002/2018GL076993

R.L. Fermo, J.F. Drake, M. Swisdak, Secondary magnetic islands generated by the Kelvin-Helmholtz instability in a reconnecting current sheet. Phys. Rev. Lett. **108**(25), 255005 (2012). https://doi.org/10.1103/PhysRevLett.108.255005

X.R. Fu, Q.M. Lu, S. Wang, The process of electron acceleration during collisionless magnetic reconnection. Phys. Plasmas **13**(1), 012309 (2006). https://doi.org/10.1063/1.2164808

H.S. Fu, Y.V. Khotyaintsev, M. André, A. Vaivads, Fermi and betatron acceleration of suprathermal electrons behind dipolarization fronts: fermi versus betatron behind DF. Geophys. Res. Lett. (2011). https://doi.org/10.1029/2011GL048528

H.S. Fu, Y.V. Khotyaintsev, A. Vaivads, M. André, S.Y. Huang, Occurrence rate of earthward-propagating dipolarization fronts: occurrence rate of DFS. Geophys. Res. Lett. (2012). https://doi.org/10.1029/2012GL051784

H.S. Fu, Yu.V. Khotyaintsev, A. Vaivads, A. Retinò, M. André, Energetic electron acceleration by unsteady magnetic reconnection. Nat. Phys. **9**(7), 426–430 (2013). https://doi.org/10.1038/nphys2664

H.S. Fu, J.B. Cao, C.M. Cully, Y.V. Khotyaintsev, A. Vaivads, V. Angelopoulos et al., Whistler-mode waves inside flux pileup region: Structured or unstructured?: Whistlers inside FPR. J. Geophys. Res. Space Physics **119**(11), 9089–9100 (2014). https://doi.org/10.1002/2014JA020204

K. Fujimoto, Wave activities in separatrix regions of magnetic reconnection. Geophys. Res. Lett. **41**(8), 2721–2728 (2014). https://doi.org/10.1002/2014GL059893

K. Fujimoto, R.D. Sydora, Plasmoid-induced turbulence in collisionless magnetic reconnection. Phys. Rev. Lett. **109**(26), 265004 (2012). https://doi.org/10.1103/PhysRevLett.109.265004

S.P. Gary, H. Karimabadi, Linear theory of electron temperature anisotropy instabilities: whistler, mirror, and Weibel. J. Geophys. Res. **111**(A11), A11224 (2006). https://doi.org/10.1029/2006JA011764

K.J. Genestreti, Y.-H. Liu, T.-D. Phan, R.E. Denton, R.B. Torbert, J.L. Burch et al., Multiscale coupling during magnetopause reconnection: interface between the electron and ion diffusion regions. J. Geophys. Res. Space Phys. (2020). https://doi.org/10.1029/2020JA027985

R.G. Giovanelli, A theory of chromospheric flares. Nature **158**(4003), 81–82 (1946). https://doi.org/10.1038/158081a0

M.V. Goldman, G. Lapenta, D.L. Newman, S. Markidis, H. Che, Jet deflection by very weak guide fields during magnetic reconnection. Phys. Rev. Lett. **107**(13), 135001 (2011). https://doi.org/10.1103/PhysRevLett.107.135001

D.B. Graham, Yu.V. Khotyaintsev, A. Vaivads, M. André, Electrostatic solitary waves with distinct speeds associated with asymmetric reconnection. Geophys. Res. Lett. **42**(2), 215–224 (2015). https://doi.org/10.1002/2014GL062538

D.B. Graham, A. Vaivads, Yu.V. Khotyaintsev, M. André, Whistler emission in the separatrix regions of asymmetric magnetic reconnection: whistlers in asymmetric separatrices. J. Geophys. Res. Space Phys. **121**(3), 1934–1954 (2016). https://doi.org/10.1002/2015JA021239

D.B. Graham, Yu.V. Khotyaintsev, A. Vaivads, C. Norgren, M. André, J.M. Webster et al., Instability of agyrotropic electron beams near the electron diffusion region. Phys. Rev. Lett. **119**(2), 025101 (2017a). https://doi.org/10.1103/PhysRevLett.119.025101

D.B. Graham, Yu.V. Khotyaintsev, C. Norgren, A. Vaivads, M. André, S. Toledo-Redondo et al., Lower hybrid waves in the ion diffusion and magnetospheric inflow regions. J. Geophys. Res. Space Phys. **122**(1), 517–533 (2017b). https://doi.org/10.1002/2016JA023572

C.T. Haynes, D. Burgess, E. Camporeale, T. Sundberg, Electron vortex magnetic holes: a nonlinear coherent plasma structure. Phys. Plasmas **22**(1), 012309 (2015). https://doi.org/10.1063/1.4906356

M. Hesse, P.A. Cassak, Magnetic reconnection in the space sciences: past, present, and future. J. Geophys. Res. Space Phys. (2020). https://doi.org/10.1029/2018JA025935

M. Hesse, K. Schindler, J. Birn, M. Kuznetsova, The diffusion region in collisionless magnetic reconnection. Phys. Plasmas **6**, 1781 (1999)

M. Hesse, N. Aunai, D. Sibeck, J. Birn, On the electron diffusion region in planar, asymmetric, systems: diffusion region in asymmetric systems. Geophys. Res. Lett. **41**(24), 8673–8680 (2014). https://doi.org/10.1002/2014GL061586

S.Y. Huang, M. Zhou, F. Sahraoui, X.H. Deng, Y. Pang, Z.G. Yuan et al., Wave properties in the magnetic reconnection diffusion region with high β: application of the k-filtering method to Cluster multispacecraft data: waves in reconnection region. J. Geophys. Res. Space Phys. (2010). https://doi.org/10.1029/2010JA015335

S.Y. Huang, A. Vaivads, Y.V. Khotyaintsev, M. Zhou, H.S. Fu, A. Retinò et al., Electron acceleration in the reconnection diffusion region: cluster observations: electron acceleration observations. Geophys. Res. Lett. (2012a). https://doi.org/10.1029/2012aGL051946

S.Y. Huang, M. Zhou, X.H. Deng, Z.G. Yuan, Y. Pang, Q. Wei et al., Kinetic structure and wave properties associated with sharp dipolarization front observed by cluster. Ann. Geophys. **30**(1), 97–107 (2012b). https://doi.org/10.5194/angeo-30-97-2012

S.Y. Huang, H.S. Fu, Z.G. Yuan, M. Zhou, S. Fu, X.H. Deng et al., Electromagnetic energy conversion at dipolarization fronts: multispacecraft results. J. Geophys. Res. Space Phys. **120**(6), 4496–4502 (2015a). https://doi.org/10.1002/2015JA021083

C. Huang, M. Wu, Q. Lu, R. Wang, S. Wang, Electron acceleration in the dipolarization front driven by magnetic reconnection. J. Geophys. Res. Space Phys. **120**, 1759–1765 (2015b). https://doi.org/10.1002/2014JA020918

S.Y. Huang, F. Sahraoui, Z.G. Yuan, J.S. He, J.S. Zhao, O.L. Contel et al., Magnetospheric multiscale observations of electron vortex magnetic hole in the turbulent magnetosheath plasma. Astrophys. J. **836**(2), L27 (2017). https://doi.org/10.3847/2041-8213/aa5f50

H. Huang, Y. Yu, L. Dai, T. Wang, Kinetic Alfvén waves excited in two-dimensional magnetic reconnection. J. Geophys. Res. Space Phys. **123**(8), 6655–6669 (2018a). https://doi.org/10.1029/2017JA025071

S.Y. Huang, K. Jiang, Z.G. Yuan, F. Sahraoui, L.H. He, M. Zhou et al., Observations of the electron jet generated by secondary reconnection in the terrestrial magnetotail. Astrophys. J. **862**(2), 144 (2018b). https://doi.org/10.3847/1538-4357/aacd4c

S.Y. Huang, K. Jiang, Z.G. Yuan, M. Zhou, F. Sahraoui, H.S. Fu et al., Observations of flux ropes with strong energy dissipation in the magnetotail. Geophys. Res. Lett. **46**(2), 580–589 (2019). https://doi.org/10.1029/2018GL081099

S.Y. Huang, Q.Y. Xiong, L.F. Song, J. Nan, Z.G. Yuan, K. Jiang et al., Electron-only reconnection in an ion-scale current sheet at the magnetopause. Astrophys. J. **922**(1), 54 (2021). https://doi.org/10.3847/1538-4357/ac2668

K.-J. Hwang, D.G. Sibeck, E. Choi, L.-J. Chen, R.E. Ergun, Y. Khotyaintsev et al., Magnetospheric multiscale mission observations of the outer electron diffusion region. Geophys. Res. Lett. **44**(5), 2049–2059 (2017). https://doi.org/10.1002/2017GL072830

H. Ji, S. Terry, M. Yamada, R. Kulsrud, A. Kuritsyn, Y. Ren, Electromagnetic fluctuations during fast reconnection in a laboratory plasma. Phys. Rev. Lett. **92**(11), 115001 (2004). https://doi.org/10.1103/PhysRevLett.92.115001

H. Ji, R. Kulsrud, W. Fox, M. Yamada, An obliquely propagating electromagnetic drift instability in the lower hybrid frequency range: oblique electromagnetic drift instability. J. Geophys. Res. Space Phys. (2005). https://doi.org/10.1029/2005JA011188

X.-F. Ji, X.-G. Wang, W.-J. Sun, C.-J. Xiao, Q.-Q. Shi, J. Liu, Z.-Y. Pu, EMHD theory and observations of electron solitary waves in magnetotail plasmas: EMHD and SSMH. J. Geophys. Res. Space Phys. **119**(6), 4281–4289 (2014). https://doi.org/10.1002/2014JA019924

R. Jin, M. Zhou, Y. Pang, X. Deng, Y. Yi, Characteristics of turbulence driven by transient magnetic reconnection in the terrestrial magnetotail. Astrophys. J. **925**(1), 17 (2022). https://doi.org/10.3847/1538-4357/ac390c

H. Karimabadi, W. Daughton, J. Scudder, Multi-scale structure of the electron diffusion region: structure of the electron diffusion region. Geophys. Res. Lett. (2007). https://doi.org/10.1029/2007GL030306

Y. Khotyaintsev, A. Vaivads, Y. Ogawa, B. Popielawska, M. André, S. Buchert et al., Cluster observations of high-frequency waves in the exterior cusp. Ann. Geophys. **22**(7), 2403–2411 (2004). https://doi.org/10.5194/angeo-22-2403-2004

Yu.V. Khotyaintsev, C.M. Cully, A. Vaivads, M. André, C.J. Owen, Plasma jet braking: energy dissipation and nonadiabatic electrons. Phys. Rev. Lett. **106**(16), 165001 (2011). https://doi.org/10.1103/PhysRevLett.106.165001

Y.V. Khotyaintsev, D.B. Graham, C. Norgren, A. Vaivads, Collisionless magnetic reconnection and waves: progress review. Front. Astronomy Space Sci. **6**, 70 (2019). https://doi.org/10.3389/fspas.2019.00070

Yu.V. Khotyaintsev, D.B. Graham, K. Steinvall, L. Alm, A. Vaivads, A. Johlander et al., Electron heating by debye-scale turbulence in guide-field reconnection. Phys. Rev. Lett. **124**(4), 045101 (2020). https://doi.org/10.1103/PhysRevLett.124.045101

G. Lapenta, Self-feeding turbulent magnetic reconnection on macroscopic scales. Phys. Rev. Lett. **100**(23), 235001 (2008). https://doi.org/10.1103/PhysRevLett.100.235001

G. Lapenta, J. Berchem, M. Zhou, R.J. Walker, M. El-Alaoui, M.L. Goldstein et al., On the origin of the crescent-shaped distributions observed by MMS at the magnetopause. J. Geophys. Res. Space Phys. **122**(2), 2024–2039 (2017). https://doi.org/10.1002/2016JA023290

O. Le Contel, A. Roux, C. Jacquey, P. Robert, M. Berthomier, T. Chust et al., Quasi-parallel whistler mode waves observed by THEMIS during near-earth dipolarizations. Ann. Geophys. **27**(6), 2259–2275 (2009). https://doi.org/10.5194/angeo-27-2259-2009

A. Le, J. Egedal, O. Ohia, W. Daughton, H. Karimabadi, V.S. Lukin, Regimes of the electron diffusion region in magnetic reconnection. Phys. Rev. Lett. **110**(13), 135004 (2013). https://doi.org/10.1103/PhysRevLett.110.135004

A. Le, W. Daughton, L.-J. Chen, J. Egedal, Enhanced electron mixing and heating in 3-D asymmetric reconnection at the Earth's magnetopause. Geophys. Res. Lett. **44**(5), 2096–2104 (2017). https://doi.org/10.1002/2017GL072522

A. Le, W. Daughton, O. Ohia, L.-J. Chen, Y.-H. Liu, S. Wang et al., Drift turbulence, particle transport, and anomalous dissipation at the reconnecting magnetopause. Phys. Plasmas **25**(6), 062103 (2018). https://doi.org/10.1063/1.5027086

S.-S. Li, J. Liu, V. Angelopoulos, A. Runov, X.-Z. Zhou, S.A. Kiehas, Antidipolarization fronts observed by ARTEMIS. J. Geophys. Res. Space Physics **119**(9), 7181–7198 (2014). https://doi.org/10.1002/2014JA020062

W.Y. Li, D.B. Graham, Yu.V. Khotyaintsev, A. Vaivads, M. André, K. Min et al., Electron Bernstein waves driven by electron crescents near the electron diffusion region. Nat. Commun. **11**(1), 141 (2020). https://doi.org/10.1038/s41467-019-13920-w

J. Liang, Y. Lin, J.R. Johnson, X. Wang, Z. Wang, Kinetic Alfvén waves in three-dimensional magnetic reconnection. J. Geophys. Res. Space Physics **121**(7), 6526–6548 (2016). https://doi.org/10.1002/2016JA022505

J. Liu, V. Angelopoulos, A. Runov, X.-Z. Zhou, On the current sheets surrounding dipolarizing flux bundles in the magnetotail: The case for wedgelets: dipolarization front current sheet. J. Geophys. Res. Space Phys. **118**(5), 2000–2020 (2013a). https://doi.org/10.1002/jgra.50092

Y.-H. Liu, W. Daughton, H. Karimabadi, H. Li, V. Roytershteyn, Bifurcated structure of the electron diffusion region in three-dimensional magnetic reconnection. Phys. Rev. Lett. **110**(26), 265004 (2013b). https://doi.org/10.1103/PhysRevLett.110.265004

Y.-H. Liu, W. Daughton, H. Karimabadi, H. Li, S.P. Gary, Do dispersive waves play a role in collisionless magnetic reconnection? Phys. Plasmas **21**(2), 022113 (2014). https://doi.org/10.1063/1.4865579

C.M. Liu, H.S. Fu, Y. Xu, J.B. Cao, W.L. Liu, Explaining the rolling-pin distribution of suprathermal electrons behind dipolarization fronts: rolling pin distribution behind DF. Geophys. Res. Lett. **44**(13), 6492–6499 (2017). https://doi.org/10.1002/2017GL074029

C.M. Liu, H.S. Fu, A. Vaivads, Y.V. Khotyaintsev, D.J. Gershman, K.-J. Hwang et al., Electron jet detected by MMS at dipolarization front. Geophys. Res. Lett. **45**(2), 556–564 (2018a). https://doi.org/10.1002/2017GL076509

C.M. Liu, H.S. Fu, Y. Xu, Y.V. Khotyaintsev, J.L. Burch, R.E. Ergun et al., Electron-scale measurements of dipolarization front. Geophys. Res. Lett. **45**(10), 4628–4638 (2018b). https://doi.org/10.1029/2018GL077928

C.M. Liu, A. Vaivads, Y.V. Khotyaintsev, H.S. Fu, D.B. Graham, K. Steinvall et al., Cross-scale dynamics driven by plasma jet braking in space. Astrophys. J. **926**(2), 198 (2022). https://doi.org/10.3847/1538-4357/ac4979

N.F. Loureiro, A.A. Schekochihin, S.C. Cowley, Instability of current sheets and formation of plasmoid chains. Phys. Plasmas **14**(10), 100703 (2007). https://doi.org/10.1063/1.2783986

S. Lu, Q. Lu, Y. Lin, X. Wang, Y. Ge, R. Wang et al., Dipolarization fronts as earthward propagating flux ropes: a three-dimensional global hybrid simulation. J. Geophys. Res. Space Phys. **120**(8), 6286–6300 (2015). https://doi.org/10.1002/2015JA021213

S. Lu, R. Wang, Q. Lu, V. Angelopoulos, R. Nakamura, A.V. Artemyev et al., Magnetotail reconnection onset caused by electron kinetics with a strong external driver. Nat. Commun. **11**(1), 5049 (2020). https://doi.org/10.1038/s41467-020-18787-w

H.Y. Man, M. Zhou, X.H. Deng, H.S. Fu, Z.H. Zhong, Z.Z. Chen et al., In situ observation of magnetic reconnection between an earthward propagating flux rope and the geomagnetic field. Geophys. Res. Lett. **45**(17), 8729–8737 (2018). https://doi.org/10.1029/2018GL079778

H. Man, Z. Zhong, H. Li, Internal structures of the ion-scale flux rope associated with dayside magnetopause reconnection. Astrophys. Space Sci. **365**(5), 87 (2020). https://doi.org/10.1007/s10509-020-03803-8

M.E. Mandt, R.E. Denton, J.F. Drake, Transition to whistler mediated magnetic reconnection. Geophys. Res. Lett. **21**(1), 73–76 (1994). https://doi.org/10.1029/93GL03382

M.B. Moldwin, W.J. Hughes, Observations of earthward and tailward propagating flux rope plasmoids: expanding the plasmoid model of geomagnetic substorms. J. Geophys. Res. **99**(A1), 183 (1994). https://doi.org/10.1029/93JA02102

F.S. Mozer, Criteria for and statistics of electron diffusion regions associated with subsolar magnetic field reconnection. J. Geophys. Res. **110**(A12), A12222 (2005). https://doi.org/10.1029/2005JA011258

F.S. Mozer, S.D. Bale, T.D. Phan, Evidence of diffusion regions at a subsolar magnetopause crossing. Phys. Rev. Lett. **89**(1), 015002 (2002). https://doi.org/10.1103/PhysRevLett.89.015002

F.S. Mozer, M. Wilber, J.F. Drake, Wave associated anomalous drag during magnetic field reconnection. Phys. Plasmas **18**(10), 102902 (2011). https://doi.org/10.1063/1.3647508

T. Nagai, I. Shinohara, M. Fujimoto, A. Matsuoka, Y. Saito, T. Mukai, Construction of magnetic reconnection in the near-Earth magnetotail with Geotail. J. Geophys. Res. **116**, A04222 (2011). https://doi.org/10.1029/2010JA016283

R. Nakamura, W. Baumjohann, B. Klecker, Y. Bogdanova, A. Balogh, H. Rème et al., Motion of the dipolarization front during a flow burst event observed by cluster: dipolarization and flow bursts. Geophys. Res. Lett. **29**(20), 3-1-3–4 (2002). https://doi.org/10.1029/2002GL015763

M. Øieroset, R.P. Lin, T.D. Phan, D.E. Larson, S.D. Bale, Evidence for electron acceleration up to ~ 300 k e V in the magnetic reconnection diffusion region of earth's magnetotail. Phys. Rev. Lett. **89**(19), 195001 (2002). https://doi.org/10.1103/PhysRevLett.89.195001

M. Øieroset, T.D. Phan, C. Haggerty, M.A. Shay, J.P. Eastwood, D.J. Gershman et al., MMS observations of large guide field symmetric reconnection between colliding reconnection jets at the center of a magnetic flux rope at the magnetopause. Geophys. Res. Lett. **43**(11), 5536–5544 (2016). https://doi.org/10.1002/2016GL069166

M. Oka, T.-D. Phan, S. Krucker, M. Fujimoto, I. Shinohara, Electron acceleration by multi-island coalescence. Astrophys. J. **714**(1), 915–926 (2010a). https://doi.org/10.1088/0004-637X/714/1/915

M. Oka, M. Fujimoto, I. Shinohara, T.D. Phan, "Island surfing" mechanism of electron acceleration during magnetic reconnection: island surfing during reconnection. J. Geophys. Res. Space Phys. (2010b). https://doi.org/10.1029/2010bJA015392

E.N. Parker, Sweet's mechanism for merging magnetic fields in conducting fluids. J. Geophys. Res. **62**(4), 509–520 (1957). https://doi.org/10.1029/JZ062i004p00509

H.E. Petschek, Magnetic annihilation, in AAS-NASA symposium on the physics of solar flares. NASA Spec. Publ. **SP-50**, 425 (1964)

T.D. Phan, L.M. Kistler, B. Klecker, G. Haerendel, G. Paschmann, B.U.Ö. Sonnerup et al., Extended magnetic reconnection at the Earth's magnetopause from detection of bi-directional jets. Nature **404**(6780), 848–850 (2000). https://doi.org/10.1038/35009050

T.D. Phan, J.F. Drake, M.A. Shay, F.S. Mozer, J.P. Eastwood, Evidence for an elongated (> 60 ion skin depths) electron diffusion region during fast magnetic reconnection. Phys. Rev. Lett. **99**(25), 255002 (2007). https://doi.org/10.1103/PhysRevLett.99.255002

T.D. Phan, J.P. Eastwood, P.A. Cassak, M. Øieroset, J.T. Gosling, D.J. Gershman et al., MMS observations of electron-scale filamentary currents in the reconnection exhaust and near the X line. Geophys. Res. Lett. **43**(12), 6060–6069 (2016). https://doi.org/10.1002/2016GL069212

T.D. Phan, J.P. Eastwood, M.A. Shay, J.F. Drake, B.U.Ö. Sonnerup, M. Fujimoto et al., Electron magnetic reconnection without ion coupling in Earth's turbulent magnetosheath. Nature **557**(7704), 202–206 (2018). https://doi.org/10.1038/s41586-018-0091-5

G. Poh, J.A. Slavin, S. Lu, G. Le, D.S. Ozturk, W. Sun et al., Dissipation of earthward propagating flux rope through re-reconnection with geomagnetic field: an MMS case study. J. Geophys. Res. Space Phys. **124**(9), 7477–7493 (2019). https://doi.org/10.1029/2018JA026451

O.A. Pokhotelov, O.G. Onishchenko, L. Stenflo, Physical mechanisms for electron mirror and field swelling modes. Phys. Scr. **87**(6), 065303 (2013). https://doi.org/10.1088/0031-8949/87/06/065303

L. Price, M. Swisdak, J.F. Drake, P.A. Cassak, J.T. Dahlin, R.E. Ergun, The effects of turbulence on three-dimensional magnetic reconnection at the magnetopause. Geophys. Res. Lett. **43**(12), 6020–6027 (2016). https://doi.org/10.1002/2016GL069578

P.L. Pritchett, Collisionless magnetic reconnection in a three-dimensional open system. J. Geophys. Res. Space Phys. **106**(A11), 25961–25977 (2001). https://doi.org/10.1029/2001JA000016

P.L. Pritchett, F.V. Coroniti, Y. Nishimura, The kinetic ballooning/interchange instability as a source of dipolarization fronts and auroral streamers. J. Geophys. Res. Space Phys. **119**(6), 4723–4739 (2014). https://doi.org/10.1002/2014JA019890

Z.Y. Pu, J. Raeder, J. Zhong, Y.V. Bogdanova, M. Dunlop, C.J. Xiao et al., Magnetic topologies of an in vivo FTE observed by double star/TC-1 at Earth's magnetopause. Geophys. Res. Lett. **40**(14), 3502–3506 (2013). https://doi.org/10.1002/grl.50714

Y. Ren, L. Dai, W. Li, X. Tao, C. Wang, B. Tang et al., Whistler waves driven by field-aligned streaming electrons in the near-earth magnetotail reconnection. Geophys. Res. Lett. **46**(10), 5045–5054 (2019). https://doi.org/10.1029/2019GL083283

A. Retinò, A. Vaivads, M. André, F. Sahraoui, Y. Khotyaintsev, J.S. Pickett et al., Structure of the separatrix region close to a magnetic reconnection X-line: cluster observations. Geophys. Res. Lett. **33**(6), L06101 (2006). https://doi.org/10.1029/2005GL024650

A. Retinò, D. Sundkvist, A. Vaivads, F. Mozer, M. Andre, C.J. Owen, In situ evidence of magnetic reconnection in turbulent plasma. Nat. Phys. **3**, 236–238 (2007)
A. Retinò, Exploring turbulent energy dissipation and particle energization in space plasmas: the science of THOR mission. (EGU General Assembly 2016, Vienna, Apr 2016), pp. EPSC2016–15240
B.N. Rogers, R.E. Denton, J.F. Drake, M.A. Shay, Role of dispersive waves in collisionless magnetic reconnection. Phys. Rev. Lett. **87**(19), 195004 (2001). https://doi.org/10.1103/PhysRevLett.87.195004
A. Runov, Current sheet structure near magnetic X-line observed by cluster. Geophys. Res. Lett. **30**(11), 1579 (2003). https://doi.org/10.1029/2002GL016730
A. Runov, V. Angelopoulos, M.I. Sitnov, V.A. Sergeev, J. Bonnell, J.P. McFadden et al., THEMIS observations of an earthward-propagating dipolarization front. Geophys. Res. Lett. **36**(14), L14106 (2009). https://doi.org/10.1029/2009GL038980
A. Runov, V. Angelopoulos, M. Sitnov, V.A. Sergeev, R. Nakamura, Y. Nishimura et al., Dipolarization fronts in the magnetotail plasma sheet. Planet. Space Sci. **59**(7), 517–525 (2011). https://doi.org/10.1016/j.pss.2010.06.006
C.T. Russell, R.C. Elphic, Initial ISEE magnetometer results: magnetopause observations. Space Sci. Rev. **22**, 681–715 (1978)
K. Schindler, A theory of the substorm mechanism. J. Geophys. Res. **79**(19), 2803–2810 (1974). https://doi.org/10.1029/JA079i019p02803
M.A. Shay, J.F. Drake, The role of electron dissipation on the rate of collisionless magnetic reconnection. Geophys. Res. Lett. **25**(20), 3759–3762 (1998). https://doi.org/10.1029/1998GL900036
M.A. Shay, J.F. Drake, B.N. Rogers, R.E. Denton, The scaling of collisionless, magnetic reconnection for large systems. Geophys. Res. Lett. **26**(14), 2163–2166 (1999). https://doi.org/10.1029/1999GL900481
M.A. Shay, J.F. Drake, B.N. Rogers, R.E. Denton, Alfvénic collisionless magnetic reconnection and the Hall term. J. Geophys. Res. Space Phys. **106**(A3), 3759–3772 (2001). https://doi.org/10.1029/1999JA001007
M.A. Shay, J.F. Drake, M. Swisdak, Two-scale structure of the electron dissipation region during collisionless magnetic reconnection. Phys. Rev. Lett. **99**(15), 155002 (2007). https://doi.org/10.1103/PhysRevLett.99.155002
M.A. Shay, J.F. Drake, J.P. Eastwood, T.D. Phan, Super-Alfvénic propagation of substorm reconnection signatures and poynting flux. Phys. Rev. Lett. **107**(6), 065001 (2011). https://doi.org/10.1103/PhysRevLett.107.065001
I. Silin, J. Büchner, A. Vaivads, Anomalous resistivity due to nonlinear lower-hybrid drift waves. Phys. Plasmas **12**(6), 062902 (2005). https://doi.org/10.1063/1.1927096
M.I. Sitnov, K. Schindler, Tearing stability of a multiscale magnetotail current sheet: tearing stability. Geophys. Res. Lett. (2010). https://doi.org/10.1029/2010GL042961
M.I. Sitnov, M. Swisdak, A.V. Divin, Dipolarization fronts as a signature of transient reconnection in the magnetotail: dipolarization front. J. Geophys. Res. Space Phys. (2009). https://doi.org/10.1029/2008JA013980
J.A. Slavin, R.P. Lepping, J. Gjerloev, M.L. Goldstein, D.H. Fairfield, M.H. Acuna et al., Cluster electric current density measurements within a magnetic flux rope in the plasma sheet: cluster flux rope observations. Geophys. Res. Lett. (2003). https://doi.org/10.1029/2002GL016411
L. Song, M. Zhou, Y. Yi, X. Deng, Z. Zhong, Reconnection front associated with asymmetric magnetic reconnection: particle-in-cell simulations. Astrophys. J. **881**(1), L22 (2019). https://doi.org/10.3847/2041-8213/ab3655
B.U.O. Sonnerup, Magnetic field reconnection, in *Solar System Plasma Physics*, vol. III, ed. by L.T. Lanzerotti, C.F. Kennel, E.N. Parker (North-Holland, New York, 1979), pp. 45–108
D. Sundkvist, A. Retino, A. Vaivads, S.D. Bale, Dissipation in turbulent plasma due to reconnection in thin current sheets. Phys. Rev. Lett. **99**(2), 025004 (2007)
P.A. Sweet, The neutral point theory of solar flares. Symp. Int. Astron. Union **6**, 123–134 (1958). https://doi.org/10.1017/S0074180900237704
X. Tang, C. Cattell, J. Dombeck, L. Dai, L.B. Wilson, A. Breneman, A. Hupach, THEMIS observations of the magnetopause electron diffusion region: large amplitude waves and heated electrons. Geophys. Res. Lett. **40**(12), 2884–2890 (2013). https://doi.org/10.1002/grl.50565
T. Terasawa, Hall current effect on tearing mode-instability. Geophys. Res. Lett. **10**(6), 475–478 (1983). https://doi.org/10.1029/GL010i006p00475

R.B. Torbert, J.L. Burch, B.L. Giles, D. Gershman, C.J. Pollock, J. Dorelli et al., Estimates of terms in Ohm's law during an encounter with an electron diffusion region: estimates of terms in Ohm's law. Geophys. Res. Lett. **43**(12), 5918–5925 (2016). https://doi.org/10.1002/2016GL069553

R.B. Torbert, J.L. Burch, T.D. Phan, M. Hesse, M.R. Argall, J. Shuster et al., Electron-scale dynamics of the diffusion region during symmetric magnetic reconnection in space. Science **362**(6421), 1391–1395 (2018). https://doi.org/10.1126/science.aat2998

R.A. Treumann, Origin of resistivity in reconnection. Earth Planets Space **53**(6), 453–462 (2001). https://doi.org/10.1186/BF03353256

A.Y. Ukhorskiy, K.A. Sorathia, V.G. Merkin, M.I. Sitnov, D.G. Mitchell, M. Gkioulidou, Ion trapping and acceleration at dipolarization fronts: high-resolution MHD and test-particle simulations. J. Geophys. Res. Space Phys. **123**(7), 5580–5589 (2018). https://doi.org/10.1029/2018JA025370

A. Vaivads, Cluster observations of lower hybrid turbulence within thin layers at the magnetopause. Geophys. Res. Lett. **31**(3), L03804 (2004). https://doi.org/10.1029/2003GL018142

A. Vaivads, Y. Khotyaintsev, M. André, A. Retinò, S. Buchert, B. Rogers et al., Structure of the magnetic reconnection diffusion region from four-spacecraft observations. Phys. Rev. Lett. **93**(10), 105001 (2004). https://doi.org/10.1103/PhysRevLett.93.105001

R. Wang, Q. Lu, A. Du, S. Wang, *In situ* observations of a secondary magnetic island in an ion diffusion region and associated energetic electrons. Phys. Rev. Lett. **104**(17), 175003 (2010). https://doi.org/10.1103/PhysRevLett.104.175003

R. Wang, Q. Lu, R. Nakamura, C. Huang, A. Du, F. Guo et al., Coalescence of magnetic flux ropes in the ion diffusion region of magnetic reconnection. Nat. Phys. **12**(3), 263–267 (2016). https://doi.org/10.1038/nphys3578

R. Wang, Q. Lu, R. Nakamura, W. Baumjohann, C. Huang, C.T. Russell et al., An electron-scale current sheet without bursty reconnection signatures observed in the near-earth tail. Geophys. Res. Lett. **45**(10), 4542–4549 (2018). https://doi.org/10.1002/2017GL076330

S. Wang, L. Chen, N. Bessho, M. Hesse, B.L. Giles, T.E. Moore, Ion behaviors in the reconnection diffusion region of a corrugated magnetotail current sheet. Geophys. Res. Lett. **46**(10), 5014–5020 (2019). https://doi.org/10.1029/2019GL082226

S. Wang, R. Wang, Q. Lu, H. Fu, S. Wang, Direct evidence of secondary reconnection inside filamentary currents of magnetic flux ropes during magnetic reconnection. Nat. Commun. **11**(1), 3964 (2020). https://doi.org/10.1038/s41467-020-17803-3

S. Wang, R. Wang, Q. Lu, C.T. Russell, R.E. Ergun, S. Wang, Large-scale parallel electric field colocated in an extended electron diffusion region during the magnetosheath magnetic reconnection. Geophys. Res. Lett. (2021). https://doi.org/10.1029/2021GL094879

J.M. Webster, J.L. Burch, P.H. Reiff, A.G. Daou, K.J. Genestreti, D.B. Graham et al., Magnetospheric multiscale dayside reconnection electron diffusion region events. J. Geophys. Res. Space Phys. **123**(6), 4858–4878 (2018). https://doi.org/10.1029/2018JA025245

J.R. Wygant, C.A. Cattell, R. Lysak, Y. Song, J. Dombeck, J. McFadden et al., Cluster observations of an intense normal component of the electric field at a thin reconnecting current sheet in the tail and its role in the shock-like acceleration of the ion fluid into the separatrix region: electric fields at the reconnection region. J. Geophys. Res. Space Phys. (2005). https://doi.org/10.1029/2004JA010708

Q.Y. Xiong, S.Y. Huang, M. Zhou, Z.G. Yuan, X.H. Deng, K. Jiang et al., Formation of negative $\mathbf{J} \cdot \mathbf{E}'$ in the outer electron diffusion region during magnetic reconnection. J. Geophys. Res. Space Phys. (2022). https://doi.org/10.1029/2022JA030264

S.T. Yao, X.G. Wang, Q.Q. Shi, T. Pitkänen, M. Hamrin, Z.H. Yao et al., Observations of kinetic-size magnetic holes in the magnetosheath. J. Geophys. Res. Space Phys. **122**(2), 1990–2000 (2017). https://doi.org/10.1002/2016JA023858

X. Yu, R. Wang, Q. Lu, C.T. Russell, S. Wang, Nonideal electric field observed in the separatrix region of a magnetotail reconnection event. Geophys. Res. Lett. **46**(19), 10744–10753 (2019). https://doi.org/10.1029/2019GL082538

S. Zenitani, M. Hesse, A. Klimas, M. Kuznetsova, New measure of the dissipation region in collisionless magnetic reconnection. Phys. Rev. Lett. **106**(19), 195003 (2011). https://doi.org/10.1103/PhysRevLett.106.195003

S. Zenitani, I. Shinohara, T. Nagai, Evidence for the dissipation region in magnetotail reconnection. Geophys. Res. Lett. **39**, L11102 (2012). https://doi.org/10.1029/2012GL051938

T.L. Zhang, Q.M. Lu, W. Baumjohann, C.T. Russell, A. Fedorov, S. Barabash et al., Magnetic reconnection in the near Venusian magnetotail. Science **336**(6081), 567–570 (2012). https://doi.org/10.1126/science.1217013

Y.C. Zhang, B. Lavraud, L. Dai, C. Wang, A. Marchaudon, L. Avanov et al., Quantitative analysis of a Hall system in the exhaust of asymmetric magnetic reconnection: hall system in asymmetric exhaust. J. Geophys. Res. Space Phys. **122**(5), 5277–5289 (2017). https://doi.org/10.1002/2016JA023620

Z.H. Zhong, R.X. Tang, M. Zhou, X.H. Deng, Y. Pang, W.R. Paterson et al., Evidence for secondary flux rope generated by the electron Kelvin-Helmholtz instability in a magnetic reconnection diffusion region. Phys. Rev. Lett. **120**(7), 075101 (2018). https://doi.org/10.1103/PhysRevLett.120.075101

Z.H. Zhong, M. Zhou, S.Y. Huang, R.X. Tang, X.H. Deng, Y. Pang, H.T. Chen, Observations of a kinetic-scale magnetic hole in a reconnection diffusion region. Geophys. Res. Lett. **46**(12), 6248–6257 (2019). https://doi.org/10.1029/2019GL082637

Z.H. Zhong, M. Zhou, R.X. Tang, X.H. Deng, D.L. Turner, I.J. Cohen et al., Direct evidence for electron acceleration within ion-scale flux rope. Geophys. Res. Lett. (2020a). https://doi.org/10.1029/2019GL085141

Z.H. Zhong, M. Zhou, R.X. Tang, X.H. Deng, Y.V. Khotyaintsev, B.L. Giles et al., Extension of the electron diffusion region in a guide field magnetic reconnection at magnetopause. Astrophys. J. **892**(1), L5 (2020b). https://doi.org/10.3847/2041-8213/ab7b7c

Z.H. Zhong, M. Zhou, X.H. Deng, L.J. Song, D.B. Graham, R.X. Tang et al., Three-dimensional electron-scale magnetic reconnection in earth's magnetosphere. Geophys. Res. Lett. (2021a). https://doi.org/10.1029/2020GL090946

Z.H. Zhong, D.B. Graham, Yu.V. Khotyaintsev, M. Zhou, O. Le Contel, R.X. Tang, X.H. Deng, Whistler and broadband electrostatic waves in the multiple X-line reconnection at the magnetopause. Geophys. Res. Lett. (2021b). https://doi.org/10.1029/2020GL091320

Z.H. Zhong, M. Zhou, Y.-H. Liu, X.H. Deng, R.X. Tang, D.B. Graham et al., Stacked electron diffusion regions and electron Kelvin-Helmholtz vortices within the ion diffusion region of collisionless magnetic reconnection. Astrophys. J. Lett. **926**(2), L27 (2022). https://doi.org/10.3847/2041-8213/ac4dee

M. Zhou, X.H. Deng, S.Y. Li, Y. Pang, A. Vaivads, H. Rème et al., Observation of waves near lower hybrid frequency in the reconnection region with thin current sheet: lower hybrid waves with reconnection. J. Geophys. Res. Space Physics (2009a). https://doi.org/10.1029/2008JA013427

M. Zhou, M. Ashour-Abdalla, X. Deng, D. Schriver, M. El-Alaoui, Y. Pang, THEMIS observation of multiple dipolarization fronts and associated wave characteristics in the near-Earth magnetotail. Geophys. Res. Lett. **36**(20), L20107 (2009b). https://doi.org/10.1029/2009GL040663

X.-Z. Zhou, V. Angelopoulos, V.A. Sergeev, A. Runov, Accelerated ions ahead of earthward propagating dipolarization fronts: dipolarization front. J. Geophys. Res. Space Phys. (2010). https://doi.org/10.1029/2010JA015481

M. Zhou, Y. Pang, X.H. Deng, Z.G. Yuan, S.Y. Huang, Density cavity in magnetic reconnection diffusion region in the presence of guide field: density cavity in reconnection. J. Geophys. Res. Space Physics (2011a). https://doi.org/10.1029/2010JA016324

M. Zhou, S. Huang, X-H. Deng, Y. Pang, Observation of sharp negative dipolarization front in the reconnection outflow region. Chin. Phys. Lett., **28**(10), 109402 (2011b)

M. Zhou, X.H. Deng, S.Y. Huang, Electric field structure inside the secondary island in the reconnection diffusion region. Phys. Plasmas **19**(4), 042902 (2012). https://doi.org/10.1063/1.3700194

M. Zhou, X. Deng, M. Ashour-Abdalla, R. Walker, Y. Pang, C. Tang et al., Cluster observations of kinetic structures and electron acceleration within a dynamic plasma bubble: observation of a dynamic bubble. J. Geophys. Res. Space Phys. **118**(2), 674–684 (2013). https://doi.org/10.1029/2012JA018323

M. Zhou, H. Li, X. Deng, S. Huang, Y. Pang, Z. Yuan et al., Characteristic distribution and possible roles of waves around the lower hybrid frequency in the magnetotail reconnection region: LHW in reconnection. J. Geophys. Res. Space Phys. **119**(10), 8228–8242 (2014a). https://doi.org/10.1002/2014JA019978

M. Zhou, X. Deng, R. Tang, Y. Pang, X. Xu, Z. Yuan, S. Huang, Evidence of deflected super-Alfvénic electron jet in a reconnection region with weak guide field: electron jet in guide field reconnection. J. Geophys. Res. Space Phys. **119**(3), 1541–1548 (2014b). https://doi.org/10.1002/2013JA019556

M. Zhou, B. Ni, S. Huang, X. Deng, M. Ashour-Abdalla, Y. Nishimura et al., Observation of large-amplitude magnetosonic waves at dipolarization fronts: MS waves at DF. J. Geophys. Res. Space Phys. **119**(6), 4335–4347 (2014c). https://doi.org/10.1002/2014JA019796

M. Zhou, M. Ashour-Abdalla, J. Berchem, R.J. Walker, H. Liang, M. El-Alaoui et al., Observation of high-frequency electrostatic waves in the vicinity of the reconnection ion diffusion region by the spacecraft of the Magnetospheric Multiscale (MMS) mission. Geophys. Res. Lett. **43**(10), 4808–4815 (2016a). https://doi.org/10.1002/2016GL069010

M. Zhou, T. Li, X. Deng, Y. Pang, X. Xu, R. Tang et al., Statistics of energetic electrons in the magnetotail reconnection. J. Geophys. Res. Space Phys. **121**(4), 3108–3119 (2016b). https://doi.org/10.1002/2015JA022085

M. Zhou, J. Berchem, R.J. Walker, M. El-Alaoui, X. Deng, E. Cazzola et al., Coalescence of macroscopic flux ropes at the subsolar magnetopause: magnetospheric multiscale observations. Phys. Rev. Lett. **119**(5), 055101 (2017). https://doi.org/10.1103/PhysRevLett.119.055101

M. Zhou, J. Berchem, R.J. Walker, M. El-Alaoui, M.L. Goldstein, G. Lapenta et al., Magnetospheric multiscale observations of an ion diffusion region with large guide field at the magnetopause: current system, electron heating, and plasma waves. J. Geophys. Res. Space Phys. **123**(3), 1834–1852 (2018a). https://doi.org/10.1002/2017JA024517

M. Zhou, M. El-Alaoui, G. Lapenta, J. Berchem, R.L. Richard, D. Schriver, R.J. Walker, Suprathermal electron acceleration in a reconnecting magnetotail: large-scale kinetic simulation. J. Geophys. Res. Space Phys. **123**(10), 8087–8108 (2018b). https://doi.org/10.1029/2018JA025502

M. Zhou, J. Huang, H.Y. Man, X.H. Deng, Z.H. Zhong, C.T. Russell et al., Electron-scale vertical current sheets in a bursty bulk flow in the terrestrial magnetotail. Astrophys. J. **872**(2), L26 (2019a). https://doi.org/10.3847/2041-8213/ab0424

M. Zhou, X.H. Deng, Z.H. Zhong, Y. Pang, R.X. Tang, M. El-Alaoui et al., Observations of an electron diffusion region in symmetric reconnection with weak guide field. Astrophys. J. **870**(1), 34 (2019b). https://doi.org/10.3847/1538-4357/aaf16f

M. Zhou, H.Y. Man, Z.H. Zhong, X.H. Deng, Y. Pang, S.Y. Huang et al., Sub-ion-scale dynamics of the ion diffusion region in the magnetotail: MMS observations. J. Geophys. Res. Space Phys. **124**(10), 7898–7911 (2019c). https://doi.org/10.1029/2019JA026817

M. Zhou, H.Y. Man, X.H. Deng, Y. Pang, Y. Khotyaintsev, G. Lapenta et al., Observations of secondary magnetic reconnection in the turbulent reconnection outflow. Geophys. Res. Lett. (2021). https://doi.org/10.1029/2020GL091215

Q.-G. Zong, Cluster observations of earthward flowing plasmoid in the tail. Geophys. Res. Lett. **31**(18), L18803 (2004). https://doi.org/10.1029/2004GL020692